

4

# A TRIDENT SCHOLAR PROJECT REPORT

NO. 159

"Evaluation of Bubble Dosimeter Response to Neutron Radiation"

AD-A216 267



UNITED STATES NAVAL ACADEMY  
ANNAPOLIS, MARYLAND

This document has been approved for public  
release and sale; its distribution is unlimited.

DTIC  
ELECTE  
JAN 02 1990  
S B D

00 01 02 061

UNCLASSIFIED

SECURITY CLASSIFICATION OF THIS PAGE (When Data Entered)

REPORT DOCUMENTATION PAGE		READ INSTRUCTIONS BEFORE COMPLETING FORM
1. REPORT NUMBER U.S.N.A. - TSPR; no. 159 (1989)	2. GOVT ACCESSION NO.	3. RECIPIENT'S CATALOG NUMBER
4. TITLE (and Subtitle) EVALUATION OF BUBBLE DOSIMETER RESPONSE TO NEUTRON RADIATION.		5. TYPE OF REPORT & PERIOD COVERED Final 1988/89
		6. PERFORMING ORG. REPORT NUMBER
7. AUTHOR(s) Eric J. Reilly		8. CONTRACT OR GRANT NUMBER(s)
9. PERFORMING ORGANIZATION NAME AND ADDRESS United States Naval Academy, Annapolis.		10. PROGRAM ELEMENT, PROJECT, TASK AREA & WORK UNIT NUMBERS
11. CONTROLLING OFFICE NAME AND ADDRESS United States Naval Academy, Annapolis.		12. REPORT DATE 7 July 1989
		13. NUMBER OF PAGES
14. MONITORING AGENCY NAME & ADDRESS (if different from Controlling Office)		15. SECURITY CLASS. (of this report)
		15a. DECLASSIFICATION/DOWNGRADING SCHEDULE
16. DISTRIBUTION STATEMENT (of this Report)  This document has been approved for public release; its distribution is UNLIMITED.		
17. DISTRIBUTION STATEMENT (of the abstract entered in Block 20, if different from Report)		
18. SUPPLEMENTARY NOTES  Accepted by the U.S. Trident Scholar Committee.		
19. KEY WORDS (Continue on reverse side if necessary and identify by block number) Dosimeters Radiation dosimetry Radiation safety measures		
20. ABSTRACT (Continue on reverse side if necessary and identify by block number)  Because of the growing concern over the consequences of neutron radiation, the U.S. Navy is seeking an enhanced capability of neutron dose measurement. Current dosimetry systems have highly non-linear responses, which can lead to under and over-response, depending on the neutron spectrum. The bubble dosimeter, which has recently been developed, appears to have strong potential because of its nearly linear energy response over a wide energy range. The  (OVER)		

DD FORM 1473  
1 JAN 73EDITION OF 1 NOV 65 IS OBSOLETE  
S/N 0102-LF-014-6601

UNCLASSIFIED

SECURITY CLASSIFICATION OF THIS PAGE (When Data Entered)

bubble dosimeter is also capable of measuring smaller neutron doses than current devices. However, very little information is available on the performance of bubble dosimetry measurement systems.

Using radiation sources at the Naval Academy, bubble dosimeters and spectrometers were irradiated under a variety of conditions. The sources used included  $\text{Cf}^{252}$ , Pu-Be, and a 14 MeV neutron generator. Results were obtained on the rate of bubble growth, detector lifetime, statistical behavior, and usefulness as a spectrometer. An evaluation of a computer enhanced optical system for reading bubble dosimeters was performed. Comparisons were also made between the bubble dosimeter and other currently accepted means of neutron dose measurement, such as the neutron rem-meter (A/N-PDR-70), NE-213, TEPC, TLD and CR-39. The studies found that the bubble dosimeter maintains constant sensitivity over 21 use cycles. The bubble dosimeter shows promise for naval dosimetry applications.

Accession For	
NTIS GRA&I	<input checked="" type="checkbox"/>
DTIC TAB	<input type="checkbox"/>
Unannounced	<input type="checkbox"/>
Justification	
By	
Distribution/	
Availability Codes	
Dist	Avail and/or Special
A-1	

U.S.N.A. - Trident Scholar project report; no. 159 (1989)

"Evaluation of Bubble Dosimeter Response to Neutron Radiation"

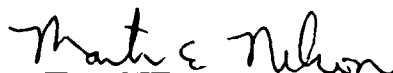
A Trident Scholar Project Report

by

Midshipman First Class Eric J. Reilly '89

U.S. Naval Academy

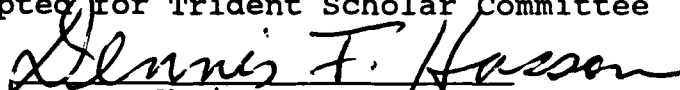
Annapolis, Maryland

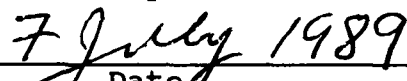


Professor Martin E. Nelson

Naval Systems Department

Accepted for Trident Scholar Committee

  
Chairperson

  
Date

USNA-1531-2

### ABSTRACT

Because of the growing concern over the consequences of neutron radiation, the U.S. Navy is seeking an enhanced capability of neutron dose measurement. Current dosimetry systems have highly non-linear responses, which can lead to under and over-response, depending on the neutron spectrum. The bubble dosimeter, which has recently been developed, appears to have strong potential because of its nearly linear energy response over a wide energy range. The bubble dosimeter is also capable of measuring smaller neutron doses than current devices. However, very little information is available on the performance of bubble dosimetry measurement systems.

Using radiation sources at the Naval Academy, bubble dosimeters and spectrometers were irradiated under a variety of conditions. The sources used included  $\text{Cf}^{252}$ , Pu-Be, and a 14 MeV neutron generator. Results were obtained on the rate of bubble growth, detector lifetime, statistical behavior, and usefulness as a spectrometer. An evaluation of a computer enhanced optical system for reading bubble dosimeters was performed. Comparisons were also made between the bubble dosimeter and other currently accepted means of neutron dose measurement, such as the neutron rem-meter (A/N-PDR-70), NE-213, TEPC, TLD, and CR-39. The studies found that the bubble dosimeter maintains constant sensitivity over 21 use cycles. The bubble dosimeter shows promise for naval dosimetry applications.

**TABLE OF CONTENTS**

Abstract. . . . .	1
1.0 Introduction . . . . .	5
2.0 Bubble Neutron Dosimetry . . . . .	10
3.0 Experimental Set-up. . . . .	23
4.0 Evaluation of Automatic Optical Reading System .	28
5.0 Initial Bubble Growth and Re-use . . . . .	35
6.0 Bubble Spectrometer Performance. . . . .	48
7.0 Detector Comparisons . . . . .	60
8.0 Conclusions and Recommendations. . . . .	64
Acknowledgements. . . . .	66
References. . . . .	67
Appendix A - The Spectral Stripping Method for BDS	
Neutron Unfolding. . . . .	70
Appendix B - Monte Carlo Neutron and Photon Transport	
Code System. . . . .	74

# LIST OF FIGURES

1.1	Radiation interaction in tissue. . . . .	6
1.2	ICRP neutron quality factors . . . . .	7
1.3	Relative responses of NTA, $\text{Np}^{237}$ , and TLD. . . . .	8
2.1	SDD acoustic bubble counter. . . . .	15
2.2	Bubble dosimeter concept . . . . .	17
2.3	Bubble dosimeter temperature dependence. . . . .	19
4.1	Optical reading of BD-100R with 21 bubbles . . . .	30
4.2	Optical reading of BD-100R with 46 bubbles . . . .	30
4.3	Optical reading of BD-100R with 66 bubbles . . . .	31
4.4	Optical reading of BD-100R with 106 bubbles. . . .	31
4.5	Optical reading of BD-100R with 154 bubbles. . . .	33
4.6	Error in optical reading system vs. enhancement. .	33
5.1	Mean bubble growth vs. time (R/3.9). . . . .	37
5.2	Mean bubble growth vs. time (R/4.7). . . . .	37
5.3	Single BD-100R bubble growth (high reading). . . .	38
5.4	Single BD-100R bubble growth (low reading) . . . .	38
5.5	Bubble growth for repeated use (R/3.9) . . . . .	39
5.6	Bubble growth for repeated use (R/4.7) . . . . .	39
5.7	Repeated use of a single BD-100R . . . . .	41
5.8	Repeated use of 6 BD-100R's (Pu-Be) (R/3.9). . . .	43
5.9	Repeated use of 6 BD-100R's (Pu-Be) (R/4.7). . . .	43
5.10	Repeated use of 6 BD-100R's ( $\text{Cf}^{252}$ ) (R/3.9). . . .	44
5.11	Repeated use of 6 BD-100R's ( $\text{Cf}^{252}$ ) (R/4.7). . . .	44

5.12	Temperature of a BD-100R . . . . .	.46
6.1	Neutron generator dose spectrum. . . . .	.51
6.2	Neutron generator fluence spectrum . . . . .	.51
6.3	BDS measured neutron doses for Cf <sup>252</sup> . . . . .	52
6.4	Cf <sup>252</sup> neutron spectrum . . . . .	53
6.5	Theoretical neutron doses for Cf <sup>252</sup> . . . . .	54
6.6	BDS unfolded neutron spectrum for Cf <sup>252</sup> . . . . .	55
6.7	BDS measured neutron doses for Pu-Be . . . . .	.56
6.8	BDS measured neutron doses for neutron generator .56	
6.9	BDS unfolded neutron spectrum for Pu-Be. . . . .	.58
6.10	BDS unfolded spectrum for neutron generator. . . .	.58

#### LIST OF TABLES

7.1	Relative responses to 14 MeV neutron generator . .	.62
7.2	Relative responses to Pu-Be neutrons . . . . .	.62
7.3	Relative responses to Cf <sup>252</sup> neutrons . . . . .	63



## 1.0 INTRODUCTION

For many years the health physics community has sought the capability to measure personal neutron dose accurately. Personal dose is a measure of the radiation damage done to human tissue, and neutron dose is the part of the dose that is caused by neutron radiation. While the amount of neutron exposure received by shipboard personnel has historically been thought to be small, recent evidence<sup>1</sup> suggests otherwise.

Because of the way in which neutrons interact with matter, and particularly human tissue, there is reason to believe that increased importance should be placed on neutron dosimetry. Neutrons deposit their energy in microscopic volumes, as opposed to gammas, which interact at the macroscopic level. The majority of neutron interactions are elastic collisions between the incident neutron and the nucleus of any given atom in the irradiated material. The nucleus is forced out of place, stripped of electrons. This is called a secondary ionization. As the ion, also known as the recoil particle, moves through the surrounding matter, it deposits its energy in a submicroscopic volume. For example, when tissue is irradiated with 1 MeV neutrons, 98 percent of the cells receive no energy. However, two percent of the cells receive fifty times the equivalent 1 MeV gamma dose.<sup>2</sup> Figure 1.1 shows this difference between gammas depositing small amounts of energy in large numbers of cells and neutron

induced recoil tracks depositing large amounts of energy in small numbers of cells. The end result is that neutrons can cause significantly more damage than their energy alone would indicate.

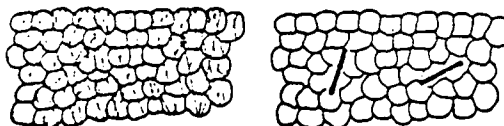


Figure 1.1 - Gamma (left) and neutron (right) interactions in tissue.

The International Commission on Radiological Protection (ICRP) accounts for the importance of neutrons by assigning a higher quality factor to neutron than gamma radiation.<sup>1</sup> A quality factor is a number which the commission has accepted as being related to the biological effects of each type of radiation. Quality factors are used in the computation of a quantity known as dose equivalent, which is the final quantity of interest in health physics. For betas and gammas of any energy, the quality factor is unity. As shown in Figure 1.2, neutron quality factors go as high as eleven and are dependent upon the energy of the incident neutrons. The non-linear energy dependence of neutron quality factors is one of the major problems in neutron dosimetry.

For a dosimeter to measure neutron dose accurately, its energy dependent response must correspond with the ICRP

neutron quality factor curve in Figure 1.2. Several attempts have been made at reproducing this ideal response, including the use of albedo thermoluminescence dosimeters (TLD), Nuclear film Type A (NTA),  $\text{Np}^{237}$  fission track dosimeters, and CR-39 foils. Of these, the TLD and NTA rely upon the measurement of energy deposition in the entire macroscopic volume of the detector material.

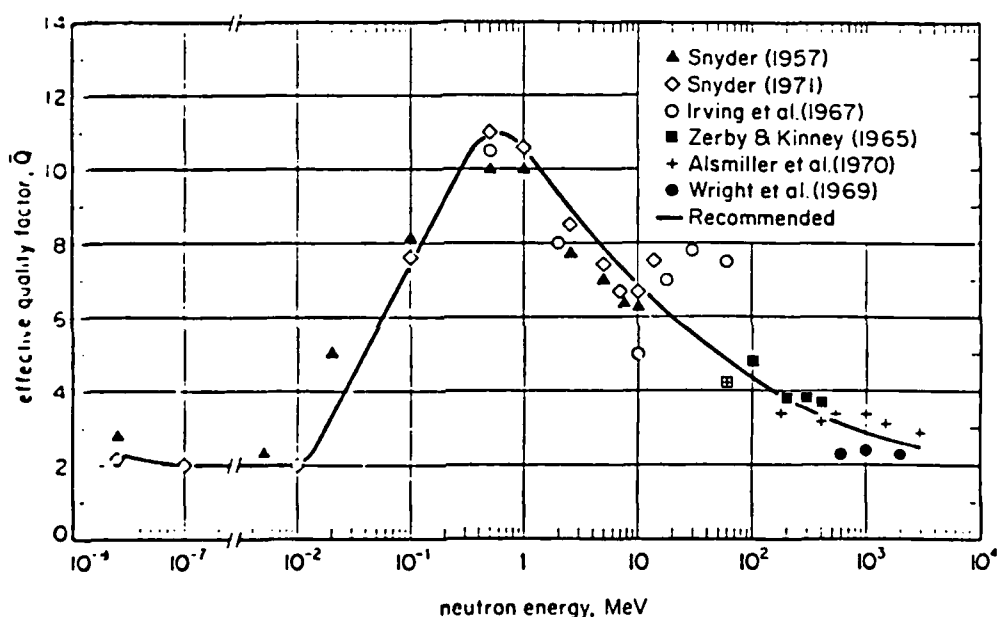


Figure 1.2 - ICRP neutron quality factors

CR-39 and  $\text{Np}^{237}$  rely upon the individual neutron interactions to produce an avalanche of effects, leading to the detection of the individual neutron tracks. For this reason they are often referred to as track damage detectors. The reason that track damage detectors work is that their energy dependent

neutron cross-sections come close to reproducing the ICRP quality factors.

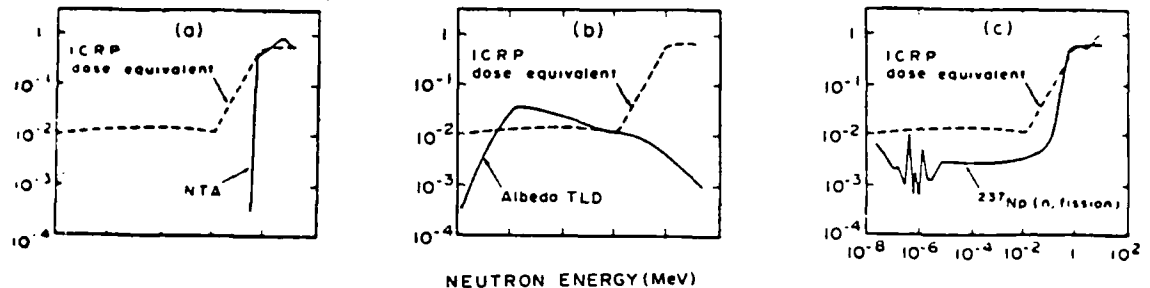


Figure 1.3 - Response of (a) NTA; (b) TLD; and (c)  $\text{Np}^{237}$

The relative responses of the NTA, TLD, and  $\text{Np}^{237}$  detectors are shown in Figure 1.3.<sup>3</sup>

While track damage detectors have shown the most promise, the two mentioned above have considerable problems.  $\text{Np}^{237}$  works well because incident neutrons induce fission in the material, creating large damage tracks. The  $\text{Np}^{237}$  fission cross-section also appears to be approximately proportional to the neutron quality factor for a wide range of energies.  $\text{Np}^{237}$ , however, is naturally radioactive and increases the wearer's overall dose.<sup>4</sup> For this reason, dosimeters containing  $\text{Np}^{237}$  are illegal in many countries. CR-39 requires an electro-chemical etching procedure to enlarge the tracks so they can be counted. The problem encountered in this procedure is that for short etch times, low energy neutron tracks appear, but high energy neutron tracks do not. If the etching time is increased, high energy tracks can be read,

but low energy tracks are severely blurred. So many parameters must be optimized in reading CR-39 that different observers often come up with large differences in reading the same dosimeter. The angle at which a neutron enters the CR-39 plays a major role in whether or not it gets detected, causing the dosimeter to give inconsistent readings in the same neutron field.<sup>1,5</sup> It has also been shown that CR-39 under-responds to both thermal and fast neutrons.

## 2.0 BUBBLE NEUTRON DOSIMETRY

Since 1952, when D.A. Glaser did his initial work with bubble chambers, it has been known that radiation could induce the formation of bubbles in a superheated liquid.<sup>6</sup> Superheated liquids have a temperature which is higher than the boiling point for their pressure, yet do not vaporize. This is a metastable state in which bubble nucleation can be triggered by air bubbles, solid impurities, or gas pockets at the solid interface. In a bubble chamber, superheating is achieved by lowering the pressure of the detector liquid. Once the pressure is lowered, bubbles begin to form at likely nucleation sites. Bubble formation and growth will continue until the system reaches the point of thermodynamic equilibrium. Particles travelling through the superheated liquid of the bubble chamber leave a trail of bubbles, but the information is unstable, and the period of operation is on the order of milliseconds. The chamber pressure can then be brought back up, all the liquid recondensed, and the chamber can be used again in the same manner. Bubble chambers have been employed as particle track detectors in particle accelerators but the concept lacked practicality for dosimetry.<sup>7,8</sup> However, recently a means has been found of applying this concept of radiation induced bubble nucleation

to the field of neutron dosimetry.

R.E. Apfel showed that liquids can be held in a viscous medium and brought to a superheated state.<sup>9</sup> Since the liquid-gel interface will not cause nucleation, small droplets of the sensitive liquid, dispersed in a viscous immiscible gel, can be held in the superheated state for indefinite periods of time. Since the bubble nucleation sites are entirely independent, the formation of one bubble will not induce the formation of another. This permits the development of a bubble detection system that does not lose stability over time. Apfel calls this the Superheated Drop Detector (SDD).

The concept behind neutron induced bubble nucleation in the SDD is that a neutron interacts with either the detector liquid or the surrounding material. This interaction produces a charged recoil particle which deposits energy in the detector liquid. The mechanism for the actual bubble nucleation is still somewhat uncertain, but the "thermal spike" model proposed by F. Seitz in 1958 is fairly well accepted.<sup>10</sup> In this model, the charged particle interacts with the electrons of other atoms, producing highly localized high temperature regions. Since the initial localized temperatures far exceed the boiling point, a bubble begins to form. If the bubble reaches a critical radius ( $R_c$ ), it will continue to grow, vaporizing the entire droplet. The critical radius ( $R_c$ ) is given by the equation:

$$R_c = 2\gamma(T)/\Delta P \quad (2.1)$$

where:

$\gamma(T)$  = Temperature dependent surface tension of the liquid at temperature T.

$\Delta P = P_v(T) + P_g - P_0$  and  $P_v(T)$  is the pressure in the bubble,  $P_g$  is the pressure of any non-condensable dissolved gas, and  $P_0$  is the external pressure.

By controlling  $\Delta P$ , the critical radius can be varied, thus varying the amount of energy required for bubble formation. There is a point where  $R_c$  is so large that beta and gamma interactions in the detector will not deposit enough local energy to form a bubble of critical size. At this point and for higher values of  $R_c$ , neutrons will still deposit enough energy to be detected. Further decreases in  $\Delta P$ , with a corresponding increase in  $R_c$ , will lead to a detector with a higher minimum neutron energy threshold. Therefore a gamma discriminating neutron detector is possible, and in fact it is possible to modify the detector to respond only to neutrons above a certain energy.

The problem of determining and relating the amount of energy a recoil particle will deposit in a given volume to the amount of energy required for bubble formation is no simple task. It is well known that the maximum amount of energy ( $E_{max}$ ) which a neutron of energy  $E_n$  can impart to a nucleus of



atomic weight  $A$  in a head-on elastic collision is given by the equation:

$$E_{\max} = 4AE_n/(A+1)^2. \quad (2.2)$$

The nucleus, which is now the recoil particle, gives up that energy along its path through the surrounding matter. The amount of energy per unit path-length ( $dE/dx$ ) that the particle gives up determines whether or not it will deposit enough energy to form a bubble. The quantity ( $dE/dx$ ) depends not only upon the particular ion, but also upon its energy. If a detector liquid is made up of several different types of atoms, the one with the highest ( $dE/dx$ ) will dominate the characteristics of the detector. The distance over which the energy deposition from the recoil particle can cause bubble nucleation is  $2R_c$ , or the critical diameter.

According to the thermal spike model, the energy dissipates very rapidly. The local high temperatures and pressures only last for times on the order of  $10^{-11}$  to  $10^{-10}$  second. During that time, a bubble must grow to critical size or else it will immediately recondense. The reversible thermodynamic work ( $W$ ) required to create a bubble of critical size can be written as:

$$W = 16\pi\gamma^3(T)/3(\Delta P)^2 \quad (2.3)$$

The energy ( $E_c$ ) deposited by the recoil particle within the critical diameter can be expressed as:

$$E_c = (dE/dx)(2R_c). \quad (2.4)$$

Then a nucleation efficiency ( $\eta$ ) can be defined as:

$$\eta = W/E_c \quad (2.5)$$

By combining equations 2.1, 2.3, and 2.4,  $\eta$  can be determined by the formula:

$$\eta = 4\pi\gamma^2/3(\Delta P)(dE/dx). \quad (2.6)$$

Based on his investigations into the values of  $(dE/dx)$  for Freon-12 ( $\text{CCl}_2\text{F}_2$ ) and Freon-114 ( $\text{C}_2\text{Cl}_2\text{F}_4$ ), Apfel has determined nucleation efficiencies on the order of three to five percent. This would indicate that much more energy than that simply required for the actual bubble formation must be deposited within the critical diameter.<sup>9</sup>

The primary reason that this bubble neutron detection system shows so much merit is that the number of bubbles produced is directly proportional to neutron dose equivalent. That is to say that when a Freon type liquid is used as the sensitive material, the detector's response roughly approximates the ICRP neutron quality factor curve over a very wide range of energies.

Apfel has developed a system that counts the bubbles as they are formed in the viscous medium. Figure 2.1 shows a schematic diagram of the SDD counting system.<sup>3</sup> As a bubble forms, the pressure wave is sensed by the transducer and recorded as an event. Knowing the rate at which bubbles are forming, the rate of neutron interaction in the detector can be determined.

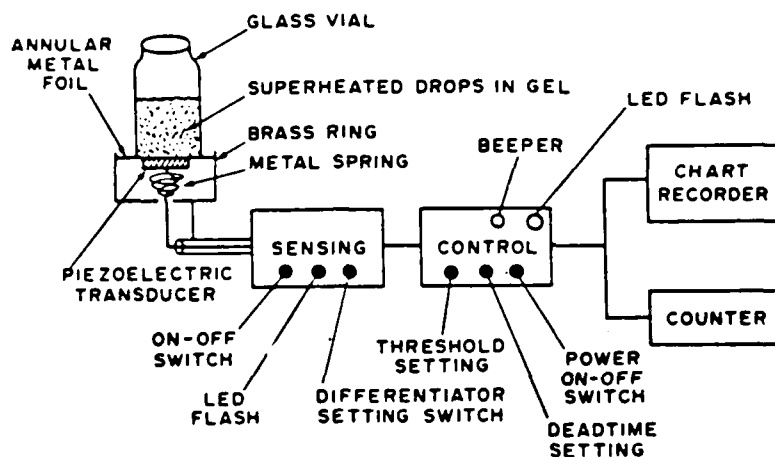


Figure 2.1 - Schematic diagram of SDD counting system.

The rate at which bubbles form,  $\phi$  (events/sec), is given by the equation:

$$\phi = \psi V \sigma(E) N_0 \rho / M \quad (2.7)$$

where:

$\psi$  = Flux (neutrons/(cm<sup>2</sup> sec))

$V$  = Total liquid volume (cm<sup>3</sup>)

$\sigma(E)$  = Neutron scattering cross-section of the liquid (cm<sup>2</sup>)

$N_0$  = Avagadro's number (atoms/mole)

$\rho$  = Liquid density (grams/cm<sup>3</sup>)

$M$  = Molecular weight (grams/mole)

Since the vaporization rate ( $\phi$ ) is a function of liquid volume, the response of the detector will decrease with time as the volume of sensitive liquid in the detector decreases.

In the monitoring system that Apfel has developed, he has taken this factor into account by estimating the volume of liquid used for each bubble counted, subtracting that volume from the previous total volume and using the new number to determine the new current detector sensitivity.

Concurrent with Apfel's work on the SDD, a team led by H. Ing at Chalk River Nuclear Laboratories in Ontario, Canada has developed a device called the bubble dosimeter.<sup>11</sup> This device is based on the same concept of a superheated Freon-type liquid drop suspended in some medium. The biggest difference between the bubble dosimeter and the SDD is the fact that the medium in which the droplets are suspended is a rigid polymer, as opposed to the gel used in the SDD. The bubble dosimeter is the first device to use a solid as the host material for a superheated liquid. This means that the bubbles formed are permanently fixed at the location where they were born. The droplets are made to be of such a size that the bubbles can be seen with the naked eye and easily counted either visually or with the aid of an optical reading system. Figure 2.2 shows the concept of the bubble dosimeter detecting neutron radiation.

The rigid medium of the bubble dosimeter is a water based polyacrylamide with salt additives. During dosimeter production, the detector liquid is injected into a monomer solution and emulsified by a mechanical agitation system.

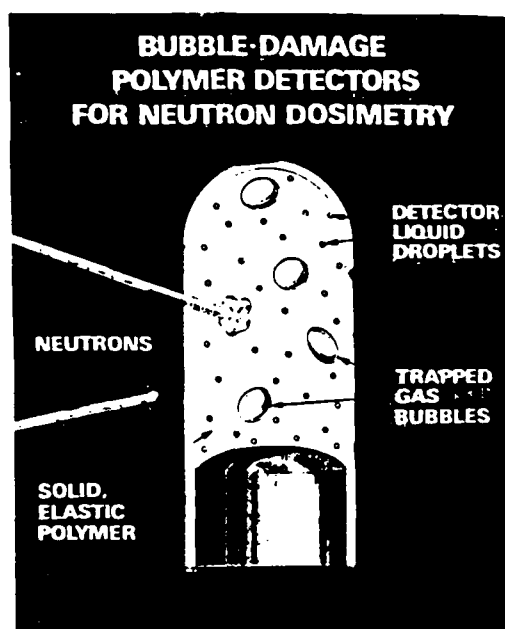


Figure 2.2 - Bubble dosimeter concept

Once the detector droplets are uniformly dispersed and of the correct size, the monomers are induced to polymerize.<sup>12</sup> An advantage of this system is that bubble dosimeters can be made in almost any shape or size. Presently, bubble dosimeters are manufactured in small plastic test tubes, primarily to keep production costs low. In the final phase of fabrication, the dosimeter is overlayed with a low boiling point liquid and capped. This increases the pressure inside the dosimeter, making it completely insensitive to radiation. In order to sensitize the dosimeter, or "turn it on," the operator simply unscrews the cap and lets the overlay quickly evaporate.

The actual chemical composition of both the detector liquid and the solid medium regulate the value of  $\Delta P$  from equation 2.1. By altering the materials, dosimeters with different detection properties can be produced. Since the

bubble dosimeter is so sensitive to changes in its chemical composition, it is important that production procedures be very strict if multiple detectors with uniform properties are required.

Once a reading has been made with the bubble dosimeter, it can be reset to zero by pressurizing it. When the dosimeter is subjected to a sufficiently high pressure, the vapor bubbles will recondense and the polymer will close in around the nucleation site. This allows the bubble dosimeter to be classified as a Class A dosimeter according to the International Organization for Standardization's (ISO) rules concerning exposure meters and dosimeters. According to the ISO, a Class A dosimeter can be read without destroying the information or the dosimeter, and can be reset to zero.<sup>13</sup>

The bubble dosimeter is currently being evaluated by several organizations, including the U.S. Navy. In the U.S. Navy, personnel are routinely exposed to neutron radiation and this exposure, or personal dose, is recorded for about 30,000 people using an albedo TLD. The shortcomings of an albedo TLD system in detecting neutrons, particularly those below 100 keV and above 2 MeV, are well known. The Navy is presently seeking to improve its neutron dosimetry capabilities.

Early research showed that the dose equivalent response of the bubble dosimeter was fairly independent of energy. This characteristic is known as a flat energy response, and effectively means that the device can at least roughly

approximate the ICRP neutron quality factor curve.<sup>14</sup> Some not so desirable behavior was also observed. Early dosimeters had sensitivities that dropped off after the first few hours of use. That problem has since been corrected in the chemical formulation of the detector. If the detector is dropped, or in some other way subjected to a mechanical shock, hundreds of tiny bubbles immediately form near the site of the impact. The most significant problem with the bubble dosimeter is its temperature dependence. Figure 2.3 shows how the relative sensitivity of the bubble dosimeter increases with temperature.

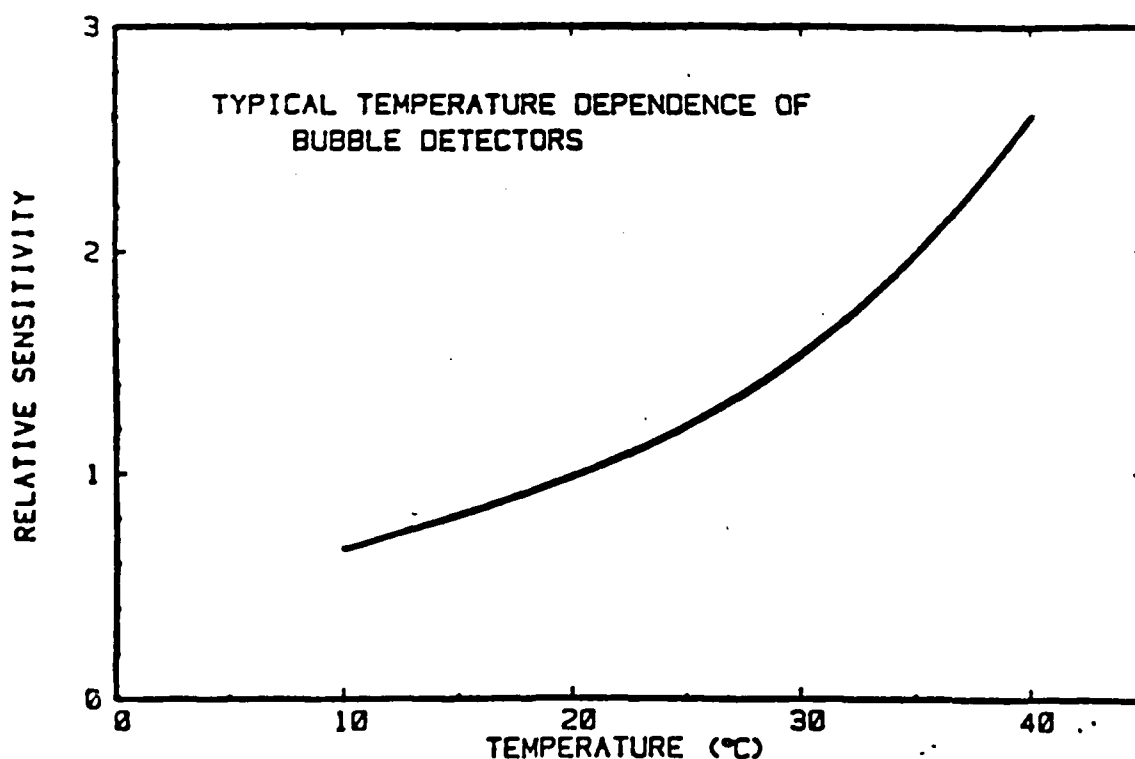


Figure 2.3 - Bubble dosimeter temperature dependence.

This amounts to a 100 percent increase in sensitivity over the temperature range of 20° to 35° C. At 48° C, the bubble dosimeter has been observed to entirely self-nucleate.<sup>15</sup> A device, currently under development at Chalk River, will mount on the end of the bubble dosimeter tube and compensate for the effect of temperature by increasing the internal pressure in the dosimeter as temperature increases.

Although the concept of just counting bubbles in a test tube seems simple, the practice has proven somewhat problematic. A person can visually count up to about 50 bubbles with reasonable accuracy. While this is somewhat tedious, it is possible. The dosimeter itself is capable of forming many hundreds of bubbles, so the limiting factor on the dynamic range at this point is the reading system. Several methods have been proposed for reading bubble dosimeters including enlarged photographs and computer driven optical counters.

Since the engineer who designs a bubble dosimeter has a certain control over the threshold energy which neutrons must have in order to be detected, it is possible to build a Bubble Detector Spectrometer (BDS). Information obtained from an effective neutron spectrometer can be extremely valuable. Spectral data can be used to compensate for the energy dependence of existing dosimetry systems, to identify an unknown neutron source, and to aid in making decisions about



various neutron shielding problems.<sup>16</sup> The U.S. Navy also desires to acquire the ability to measure neutron spectra aboard ship.

By comparing the readings from a group of threshold detectors, the neutron spectrum can be calculated through the use of an "unfolding" technique. The idea is that a detector with a high energy threshold will only respond to neutrons above its threshold. Then if a detector with a somewhat lower threshold is exposed to the same radiation, at the same time, it should respond to all neutrons above the high energy threshold, plus those between the high threshold and its threshold. The difference between the reading from the high energy dosimeter and the lower energy one would approximate the amount of the dose that was received between the two energy levels.

The ability to formulate a threshold detector requires a thorough knowledge of all the nuclear reactions which affect the response characteristics of the bubble dosimeter. For example, in addition to the type of neutron interactions described earlier; that is, the elastic collision which produces an ionization, there are other interactions taking place within the detector. Detector materials often contain chlorine, which undergoes the following nuclear reaction at low energies:  $\text{Cl}^{35} (n,p) \text{S}^{35}$ . The proton produced in this reaction has an energy of 598 keV, which is considerably more than that required for bubble nucleation. Nitrogen is a major

constituent in the rigid polymer and it undergoes,  $N^{14} (n,p)$   $C^{14}$ , which yields a 558 keV proton. The detectors containing Fluorine have also shown an interesting characteristic. The reaction  $F^{19} (n,\gamma) F^{20}$  has a resonance for 27 keV neutrons.<sup>17</sup> This means that the detector will over-respond dramatically if a substantial portion of the neutron dose is at 27 keV.

### 3.0 EXPERIMENTAL SET-UP

The experiments conducted in this project made use of the model BD-100R bubble dosimeter, and two experimental Bubble Detector Spectrometer (BDS) sets. The BD-100R and BDS dosimeters are encapsulated in small test tubes as previously described. The detector liquid is Freon and the rigid medium is a polyacrylamide. The manufacturer's listed BD-100R sensitivities ranged from 3.3 to 12 bubbles/mrem, but most of the experiments utilized dosimeters with sensitivities of either 3.9 or 4.7 bubbles/mrem.

Each of the two BDS's actually consisted of 36 dosimeters with six separate neutron energy thresholds. Only three dosimeters from each energy group were used at once, which meant that there were actually four operational spectrometers, with eighteen dosimeters each. The energy thresholds for the BDS dosimeters were 10 keV, 100 keV, 600 keV, 1.5 MeV, 2.5 MeV, and 10 MeV.

Repressurization and zeroing of the dosimeters was accomplished in a specially designed water-filled pressurizer. The pressurizer is capable of holding eighteen dosimeters and can develop pressures up to 1000 psig. Most pressurizations were done at pressures over 600 psig for several hours.

All BD-100R irradiations were made in the nucleonics

laboratory irradiation room at the United States Naval Academy, using the radiation sources normally available there. The three neutron sources used were a neutron generator, Plutonium-Beryllium (Pu-Be), and Californium ( $\text{Cf}^{252}$ ). BDS irradiations were made using the three sources at the Naval Academy, as well as a  $\text{Cf}^{252}$  source at the National Institute of Standards and Technology (NIST). The  $\text{Cf}^{252}$  at NIST was used both bare and moderated with heavy water.

The neutron generator at the Naval Academy is a Kaman Model A-711. It operates on the deuterium-tritium fusion reaction which produces monoenergetic neutrons at 14.3 MeV. The rate of neutron production is controllable and the generator is capable of producing in excess of  $10^{10}$  neutrons per second. The primary reaction in the neutron generator is given by:



The  $\text{Pu}^{239}$  in the Pu-Be source emits alphas which react with the beryllium to produce neutrons with energies between 2 and 4 MeV. Each Pu-Be source used produces approximately  $2 \times 10^6$  neutrons per second by the following reaction:



$\text{Cf}^{252}$  is a self fissioning isotope.  $\text{Cf}^{252}$  has an effective half-life of 2.646 years and produces  $2.311 \times 10^6$  neutrons per second per microgram. The neutrons produced have a relative peak energy of about 1 MeV and an average energy of 2.348 MeV.

The mass of the  $\text{Cf}^{252}$  source was approximately 0.5 micrograms during the exposures.

Exposed dosimeters were read with an optical reading system developed at Chalk River. The optical reader consists of a liquid bath, a television camera system, and a computer image enhancement and counting system. The dosimeter is immersed in the optical fluid, which was chosen for its surfactant and light transmission properties. Light enters the bath through one window and the television camera views the dosimeter through the other. The image is then processed and enhanced by the computer, in this case, a Compaq 286. The amount of enhancement done on the image is fully controlled by the operator. Once the image has been properly enhanced, the computer counts the number of bubbles. The software used for the image enhancement and counting was originally developed for the counting of cultures in petri dishes, but was modified to enable it to count bubbles in test tubes.

In conjunction with the bubble dosimeters, five major neutron detection systems were employed to measure the neutron dose and describe the relative neutron spectrum. For the measurement of neutron dose, a neutron rem-meter (A/N-PDR-70), a Tissue Equivalent Proportional Counter (TEPC), CR-39 track etch dosimeters, and albedo TLD's were employed. An NE-213 liquid scintillator was used for neutron spectroscopy as well as dose measurement.

The A/N-PDR-70 neutron rem-meter is currently the

standard means of neutron detection in the U.S. Navy. It is based on a proportional counter filled with  $\text{BF}_3$  gas, which measures the energy from neutron induced ionizations. The  $\text{BF}_3$  detector has a low efficiency for detecting high energy neutrons, so it is encased in polyethylene, which slows the incident high energy neutrons down to detectable speeds.

The TEPC was the first neutron detection system to measure energy deposition in a microscopic volume.<sup>18</sup> The heart of the TEPC is a sphere filled with a very low pressure gas which has chemical composition roughly approximating human tissue. A high voltage power supply creates a potential across the sphere. When a neutron interacts with the gas, causing ionizations, the electrons produced are collected at the anode. The energy of each event is then divided by the average chord length of the sphere to obtain lineal energy ( $dE/dx$ ). A neutron quality factor is then applied to each count based upon its lineal energy, and all neutron events are integrated to obtain the total neutron dose. The TEPC was evaluated at the U.S. Naval Academy in a previous Trident Scholar Report.<sup>19</sup>

The TLD's used were the Navy's new DT-648/PD model, supplied and read by the Naval Medical Command's Naval Dosimetry Center. The DT-648/PD has four lithium fluoride based chips, one of which is used solely for the purpose of neutron dose measurement, and is shielded by  $600 \text{ mg/cm}^2$  of plastic.<sup>20</sup> The DT-648/PD is an albedo device, which relies

upon the radiation scattered back from within the body of the wearer, as well as the directly incident radiation in order to make an accurate measurement. To account for this effect during irradiation, the TLD's were mounted on a phantom, which is a 16"x16"x6" block of plexiglas. The size of the phantom was selected in accordance with Department of Energy standards.<sup>21</sup>

The CR-39 detectors used were supplied and read by the Nevada Test Site. They were the same CR-39 dosimeters used for the routine monitoring of Department of Energy personnel engaged in neutron radiation work.

An NE-213 detector is an organic liquid scintillation counter which is capable of yielding information not only about the energy of incident radiation, but about whether the radiation is neutron or gamma. The NE-213 system in use at the U.S. Naval Academy has been described in detail by Nelson, et al,<sup>22</sup> and Fischahs.<sup>23</sup> The three parameters monitored on the NE-213 are event energy, event rise time, and number of counts. Neutron interactions in the NE-213 have longer rise times than gamma interactions, so the data are separated into gamma and neutron events. The neutron data are then unfolded to produce the neutron spectrum and the absorbed neutron dose. An ND9900 analyzer was used to process the 128x128 channels of data taken from the NE-213 detector.

#### 4.0 EVALUATION OF AUTOMATIC OPTICAL READING SYSTEM

The limitations of an average person's ability and endurance in counting bubbles in the BD-100R severely restrict the independent usefulness of the device. The absolute upper limit, in terms of the number of bubbles a person can visually count, is approximately 50. Counting small bubbles in close proximity also requires extremely high levels of concentration, making the process very labor intensive. If the bubble dosimeter is ever to be used for any large scale monitoring of neutron dose, an automated reading system will accompany it.

The performance and characteristics of the automatic reader, as described in section 3.0, were evaluated with the goal of determining its usefulness during later experiments. Optimization of the various parameters involved in the operation of the reader was also important.

The first phase of optical reader operation is the set-up procedure. During set-up the detector is aligned in the bath, and adjustments can be made to the camera aperture and focus. The dosimeter can be rotated in the bath to allow the camera to see it from different angles. Generally, the dosimeters were counted from several angles and the results were averaged. The camera must be set for minimum distance



in order to focus properly. Then the aperture is adjusted so that the images of the bubbles appear and do not bleed into each other.

Next, a computer enhancement threshold must be chosen. The amount that the computer enhances the bubble dosimeter image is the most important factor in obtaining accurate readings. When the enhancement threshold is set low, the individual bubbles appear larger than they actually are, and when it is set high, the bubbles appear smaller than they actually are. The first experiments conducted were to determine the effect of enhancement on the accuracy of the reader.

BD-100R's were irradiated with  $\text{Cf}^{252}$  for a number of irradiation times, producing between 21 and 154 bubbles. Each dosimeter was then read from eight different angles, at varying enhancement thresholds from 50 to 150. The average of these eight readings was then compared to the true number of bubbles as determined by careful visual counting and enlarged photographs. Figures 4.1 through 4.4 show how the enhancement affects the number of bubbles that the optical reader can count, for irradiations producing between 21 and 106 bubbles.

At low enhancement thresholds, effects such as dust particles and minor imperfections in the test tube were often enhanced to the point where the counting program recognized them as bubbles. This accounts for the overly high number of

## BD-100R With 21 Bubbles

30

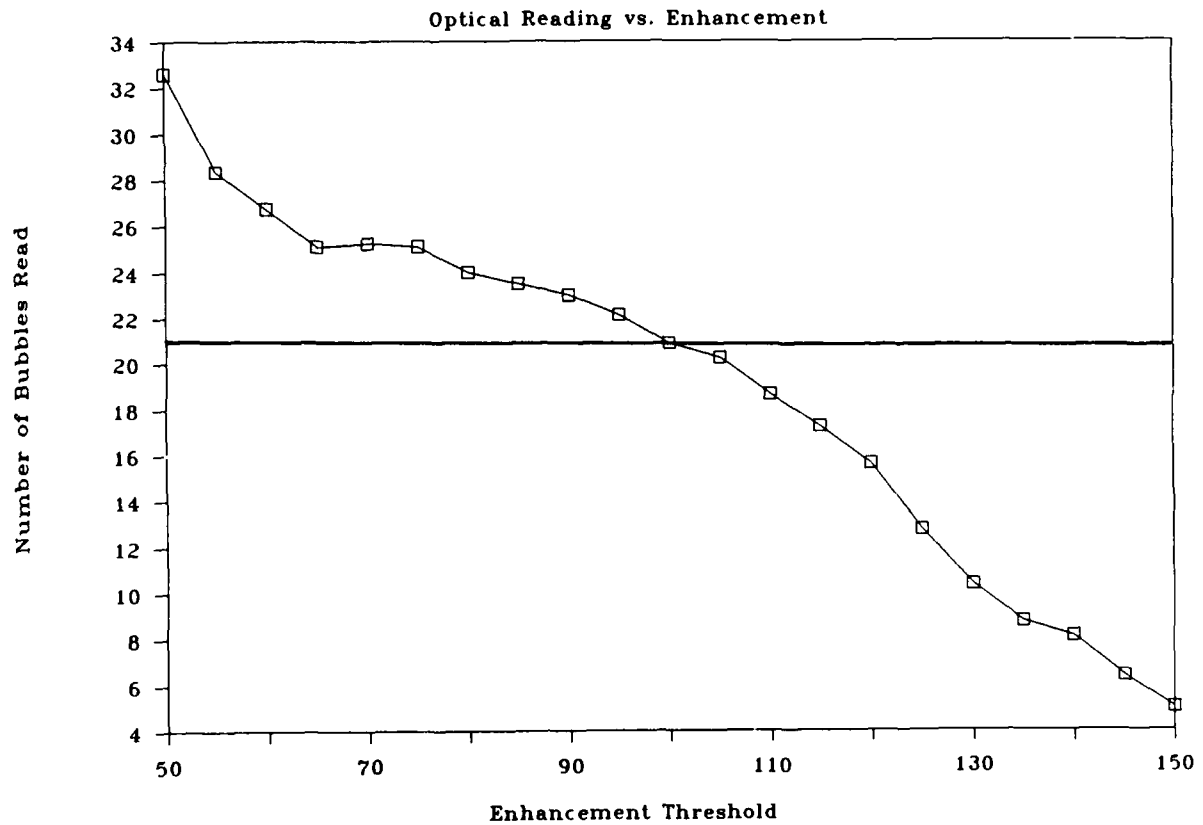


Figure 4.1 Optical Reading System Response With 21 Bubbles

## BD-100R With 46 Bubbles

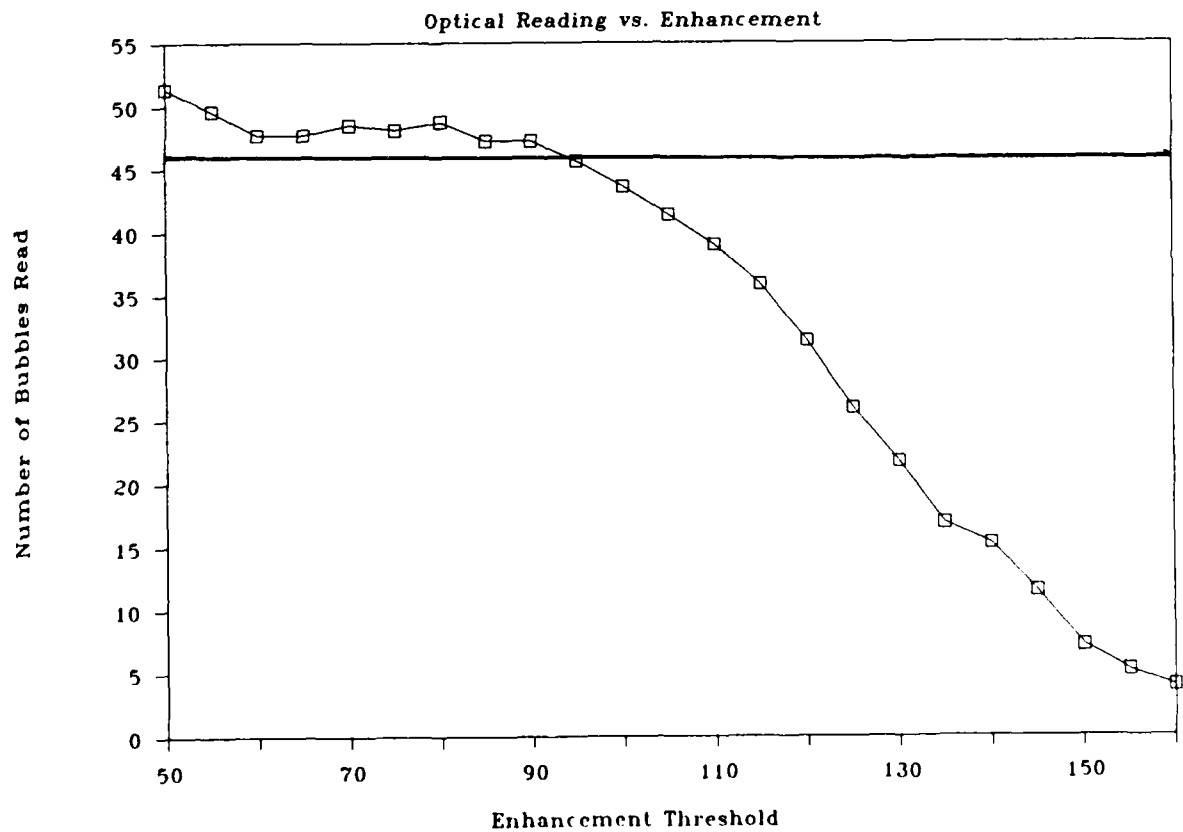


Figure 4.2 Optical Reading System Response With 46 Bubbles

## BD-100R With 66 Bubbles

31

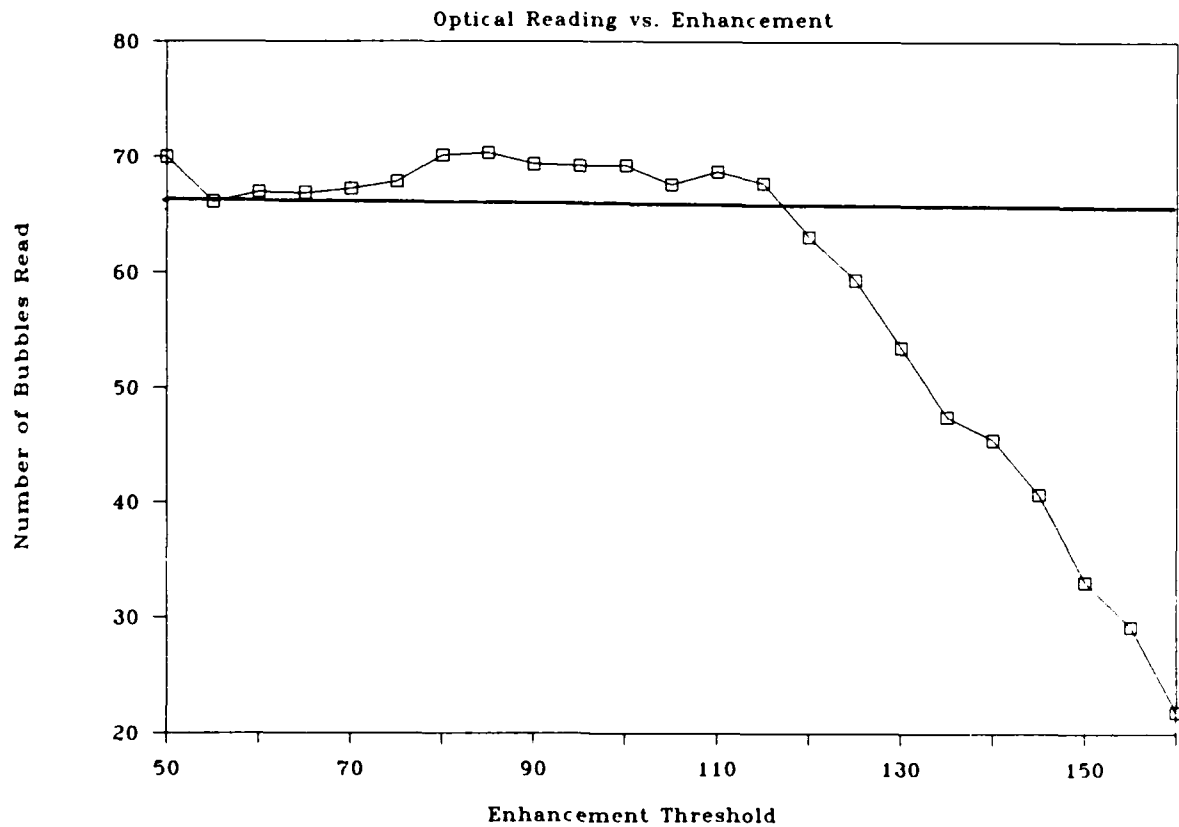


Figure 4.3 Optical Reading System Response With 66 Bubbles

## BD-100R With 106 Bubbles

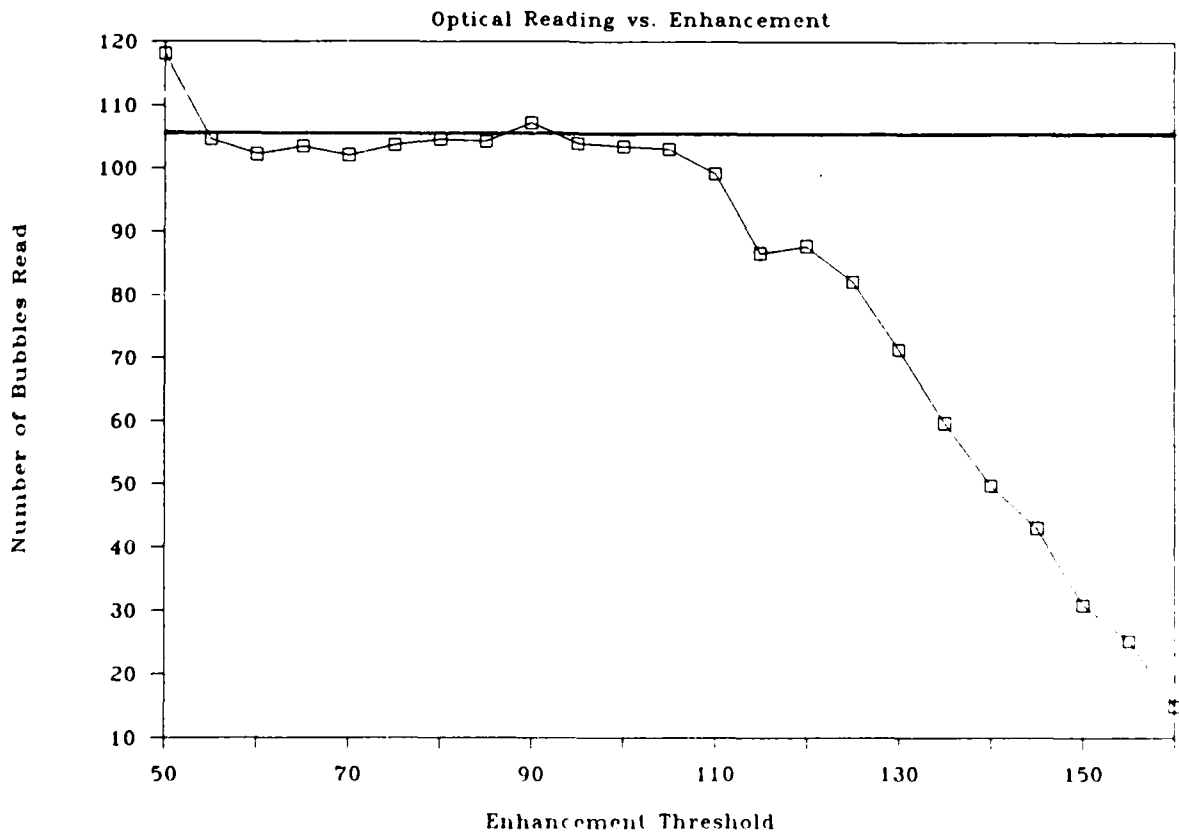


Figure 4.4 Optical Reading System Response With 106 Bubbles

counts that consistently occurred at low enhancement thresholds. As the enhancement threshold was increased, the reader will reach a point where real bubbles are eliminated from the image, causing the reading to drop below the correct value.

For the dosimeter with 154 bubbles (Figure 4.5), no usable enhancement setting yielded a reading equal to the correct value. The high reading at a threshold of 50 is not practical because at that setting, the smallest imperfections in the test tube and detector material are amplified and counted as bubbles. The otherwise consistently low readings were caused by bubbles shielding other bubbles. Therefore it was concluded that when the number of bubbles in a BD-100R exceeds about 110, the reader cannot differentiate between all of the bubbles. This places an upper limit on the exposure that a BD-100R can measure.

In order to determine the optimum enhancement threshold for general use while reading BD-100R's, the percent error was computed for each reading. Figure 4.6 shows a plot of the average percent error as a function of enhancement threshold. The enhancement threshold values of 95 and 100, giving the lowest percent reading error, were decided upon as the optimum values.

When the number of angles each dosimeter was counted from was reduced from eight to four, the results did not change significantly, but the time involved in the counting procedure

## BD-100R With 154 Bubbles

33

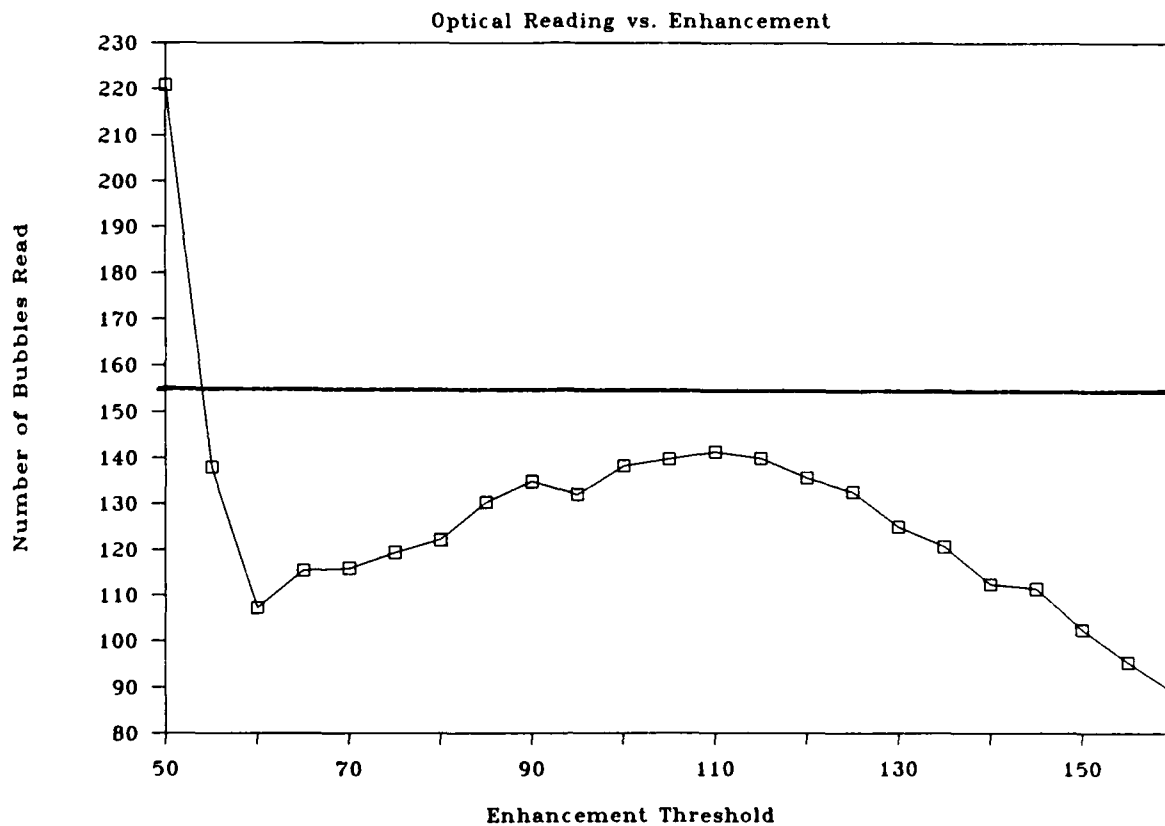


Figure 4.5 Optical Reading System Response With 154 Bubbles

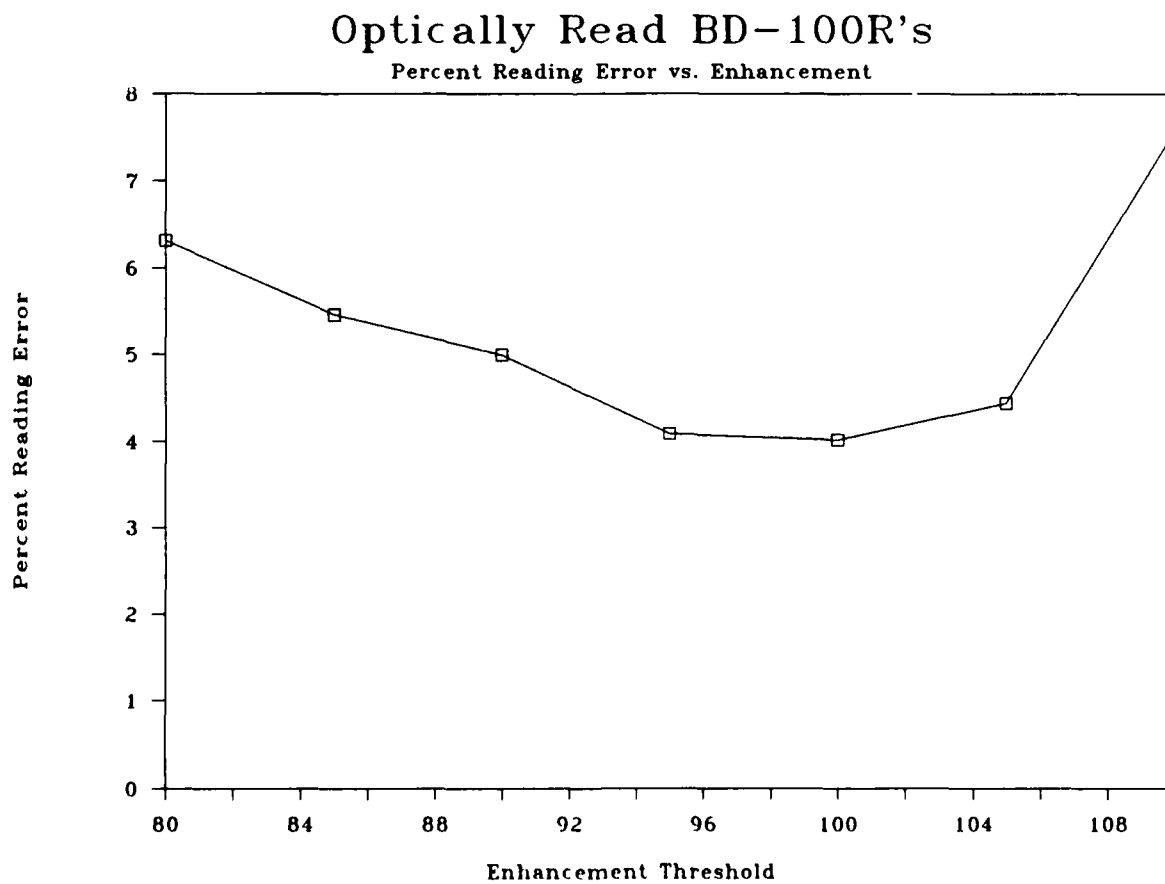


Figure 4.6 Error In Optical Reading System

was dramatically reduced. The standard procedure used for counting BD-100R's in most subsequent work has been to count and average four views at a threshold of 95 or 100.

While the use of the automatic optical reader only extends the dynamic range of the bubble dosimeter system by a factor of two, it does make possible the handling of a large number of detectors at once. The problem of bubbles obscuring other bubbles arises from the fact that the program counts the images on a two-dimensional projection of the dosimeter. A three-dimensional counting system may overcome this difficulty and significantly increase the maximum number of bubbles counted. An improved reading system is currently under development at Chalk River and the Naval Surface Warfare Center, White Oak, Maryland.

## 5.0 INITIAL BUBBLE GROWTH AND RE-USE

Although one of the claims that the manufacturer makes is that the bubbles are formed and become visible instantly upon irradiation, this was not found to be the case. While bubbles did appear during irradiation, many bubbles appeared over the first few hours following irradiation. In addition, the bubbles underwent a general growth which was greatest during the first day after irradiation and continued slowly thereafter.

It seems likely that all potential bubbles reach critical size at the time of irradiation, but simply are not large enough to be seen visually, or counted by the optical reader. Bubbles formed by larger than average energy depositions would have an initial internal pressure substantially higher than the pressure exerted by the detector medium. Therefore these bubbles would attain a significant size upon nucleation. Bubbles that are formed with just enough energy to get them up to critical size and thus prevent them from recondensing, would have an internal pressure only slightly greater than that exerted by the detector medium. As a result, these bubbles grow at an initially slower rate. This explanation of a possible mechanism is supported by the fact that bubble growth can be halted completely by adding a low boiling point

liquid to the dosimeter, thus increasing the pressure in the detector medium.

Figures 5.1 and 5.2 show the pattern of bubble growth that the BD-100R was found to follow. Each graph represents the mean response, as read by the optical reader, of six detectors exposed simultaneously to a Pu-Be source. The error bars represent plus and minus one standard deviation at each reading. In Figure 5.1 the dosimeters had a listed sensitivity of 3.9 bubbles per millirem and in Figure 5.2 they had a listed sensitivity of 4.7 bubbles per millirem. The wide error margins are due to two major effects. First, although the mean growth curves appear fairly smooth, several of the individual growth curves were not. Figures 5.3 and 5.4 show examples of how much some of the actual growth patterns varied. Second, although all of the dosimeters in each group had the same listed sensitivity, the actual sensitivities varied widely. This was found to be a common problem and the results of re-use experiments yielded a more complete explanation of this characteristic.

Figures 5.5 and 5.6 show the mean bubble growth patterns of six BD-100R's over four use cycles. All irradiations were of the same duration, and done with the same Pu-Be source, under almost identical conditions. Since all of the curves follow the same basic pattern and no general trends are apparent, this seems to indicate that the number of times a BD-100R has been used does not significantly affect the way



# BD-100R Bubble Growth (R/3.9)

37

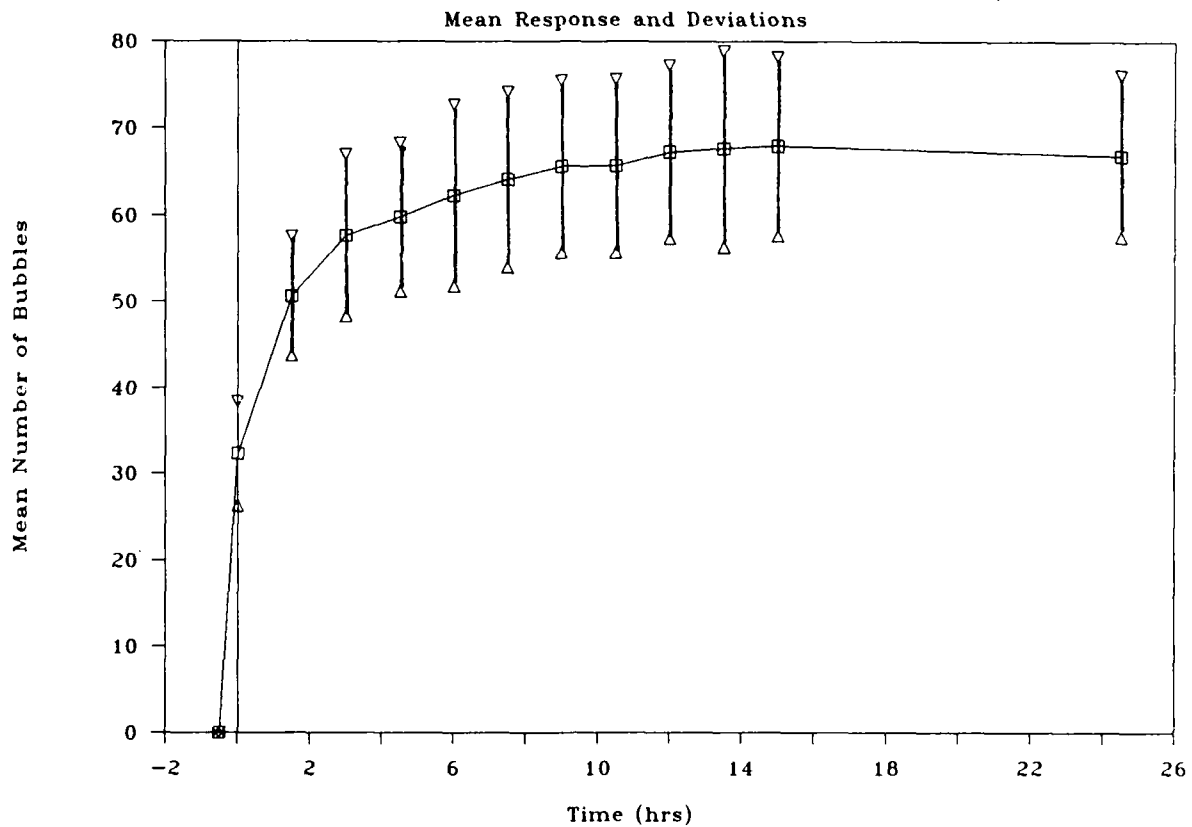


Figure 5.1 Mean Bubble Growth Versus Time (R/3.9)

# BD-100R Bubble Growth (R/4.7)

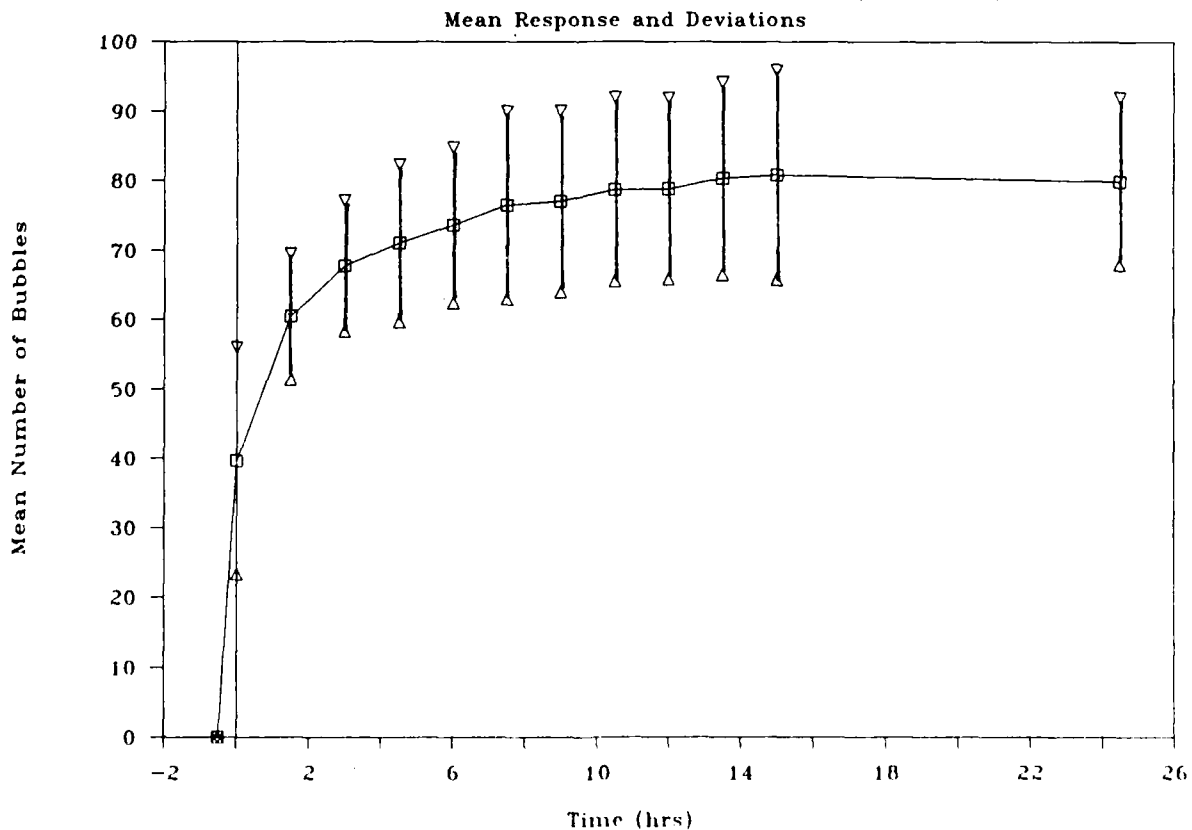


Figure 5.2 Mean Bubble Growth Versus Time (R/4.7)

## Single BD-100R Bubble Growth

38

Initial Reading is Close to Final

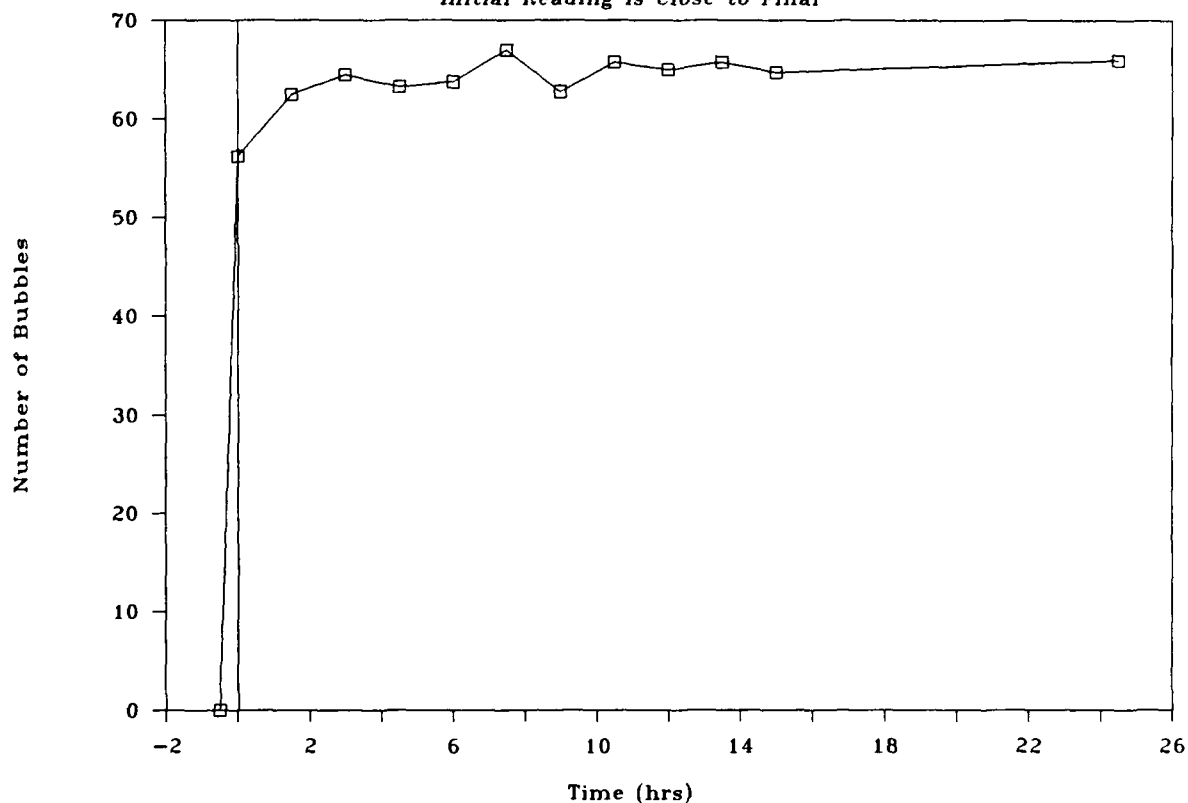


Figure 5.3 Single BD-100R Bubble Growth (high reading)

## Single BD-100R Bubble Growth

Initial Reading is Less Than Final

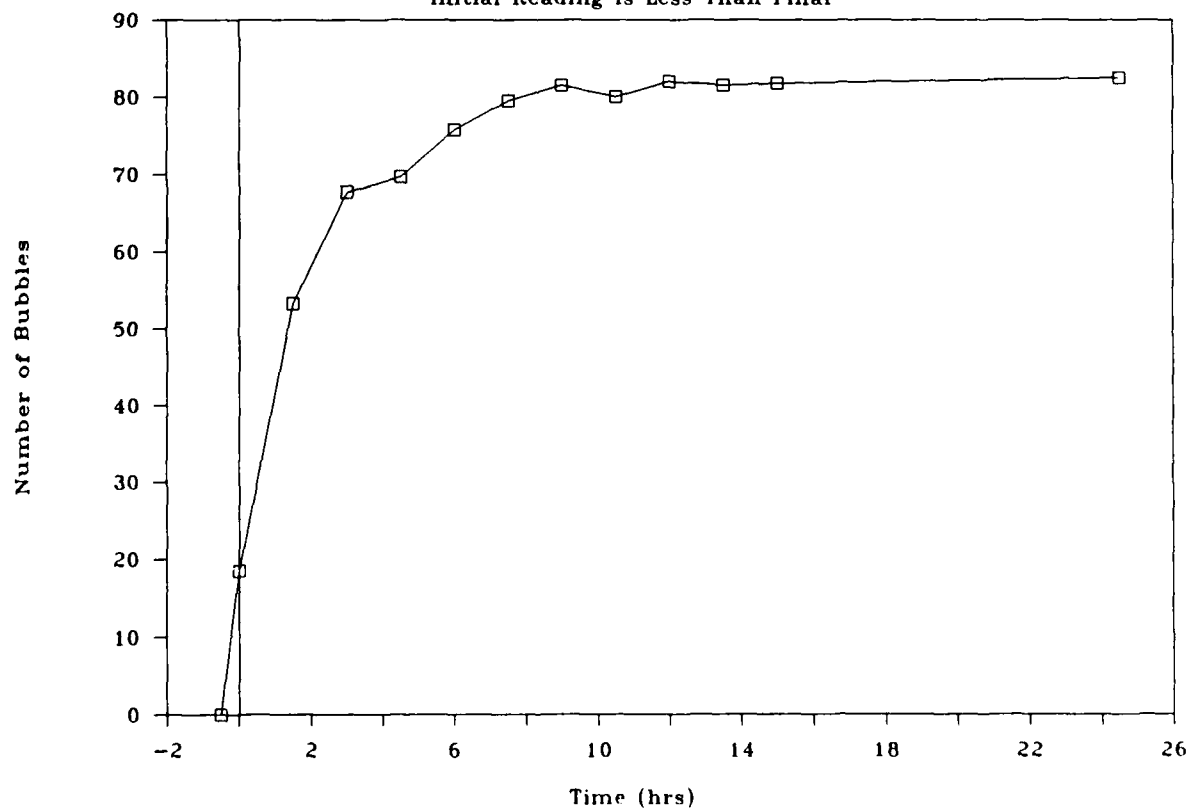


Figure 5.4 Single BD-100R Bubble Growth (low reading)

# Bubble Growth for Repeated Use (R/3.9) 39

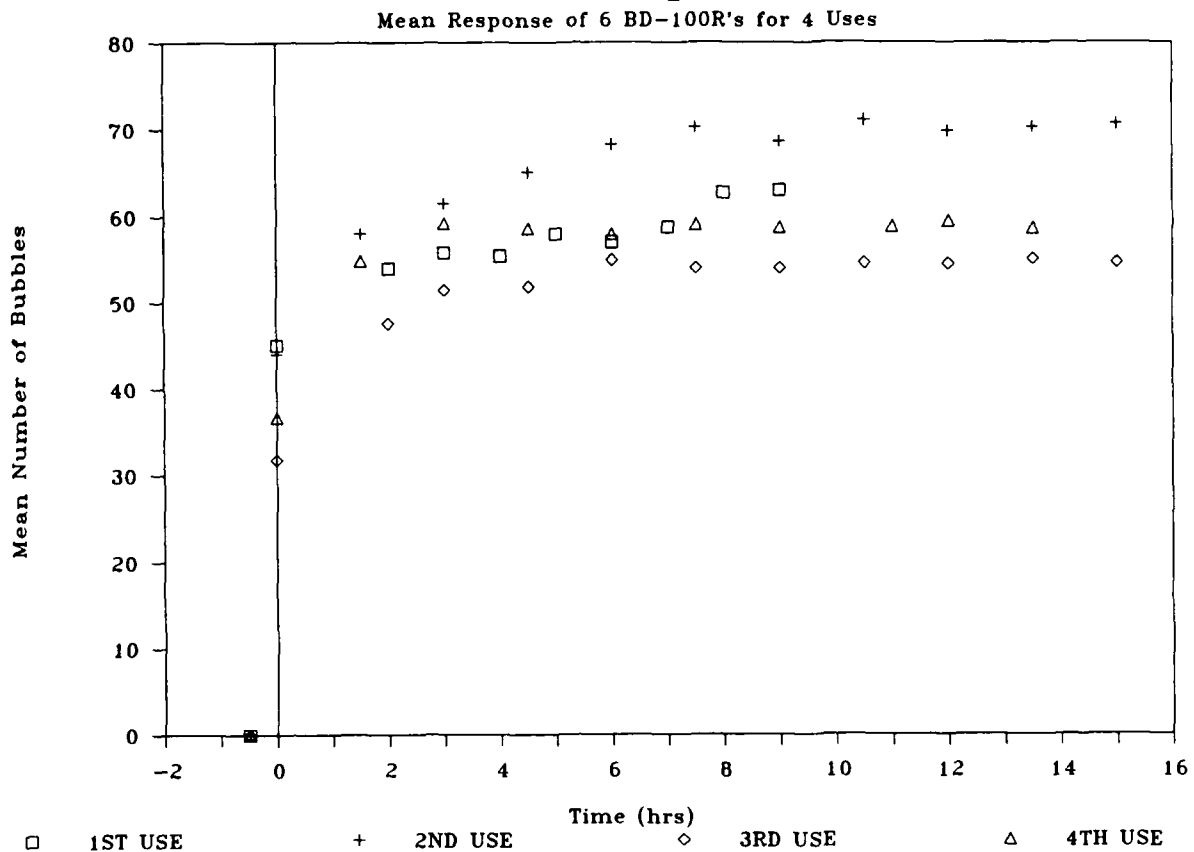


Figure 5.5 Bubble Growth For Repeated Use (R/3.9)

# Bubble Growth for Repeated Use (R/4.7)

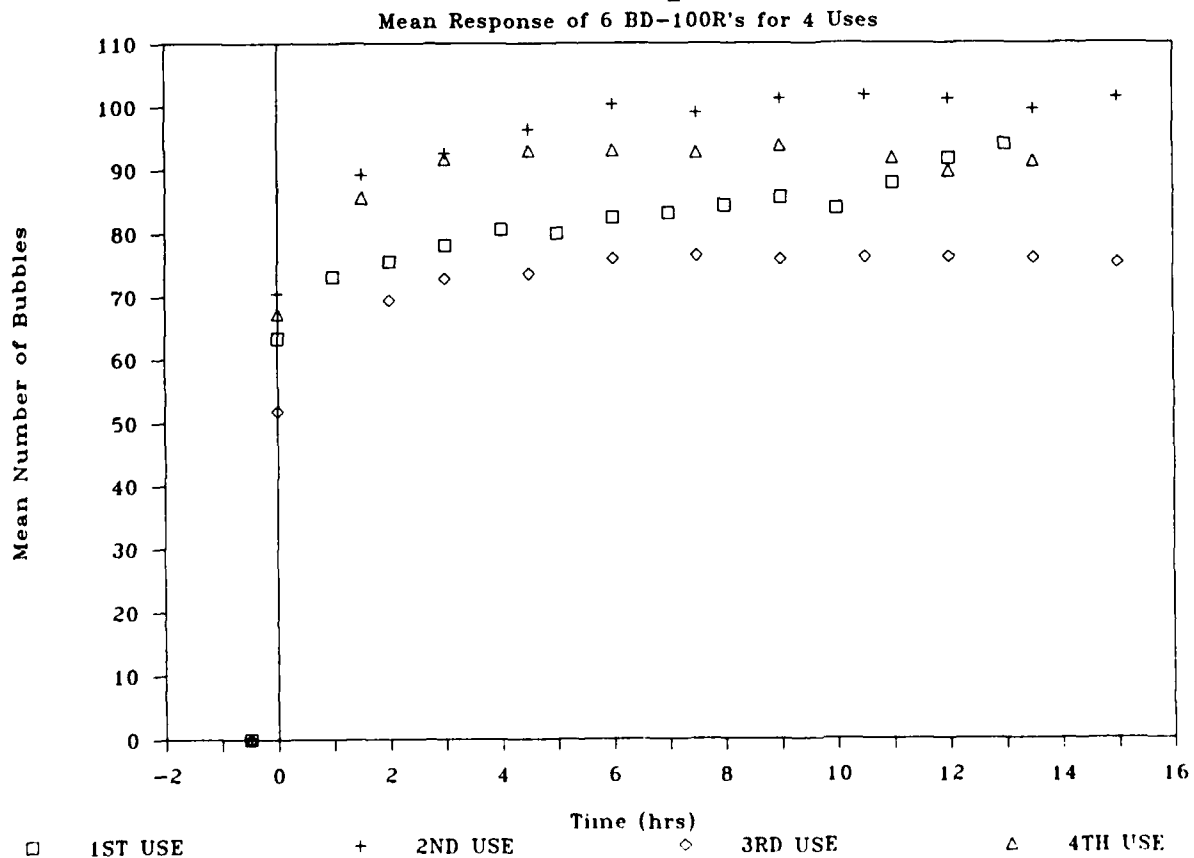


Figure 5.6 Bubble Growth For Repeated Use (R/4.7)

its bubbles grow.

The primary result of the information obtained in the bubble growth studies is the fact that it takes about fifteen hours for the BD-100R reading to stabilize. Operationally this is important because the delay time must be taken into account whenever the user intends to make an accurate dose measurement. From a personnel dosimetry viewpoint, this means that a person wearing the BD-100R would not be able to see his full neutron dose immediately. This is not a severe problem because the bubble dosimeter is so sensitive that it does give some response immediately. If a person were to be exposed to any significantly dangerous amount of neutron radiation, the bubble dosimeter would provide adequate initial indication of the danger.

One of the most important characteristics of any radiation detection system is the manner in which that system responds to the same radiation field when numerous readings are taken. In order to determine these characteristics for the BD-100R, 12 dosimeters were exposed to the same Pu-Be source 21 times and 12 more dosimeters were exposed to the same Cf<sup>252</sup> source 14 times.

Figure 5.7 shows the response of a single dosimeter to the same Pu-Be field over 21 use cycles. This performance is clearly indicative of a well behaved detection system. The deviations between the individual readings are relatively small and can be accounted for by the statistical nature of

radiation. A similar response was found for the bubble dosimeters exposed to the  $\text{Cf}^{252}$  source.

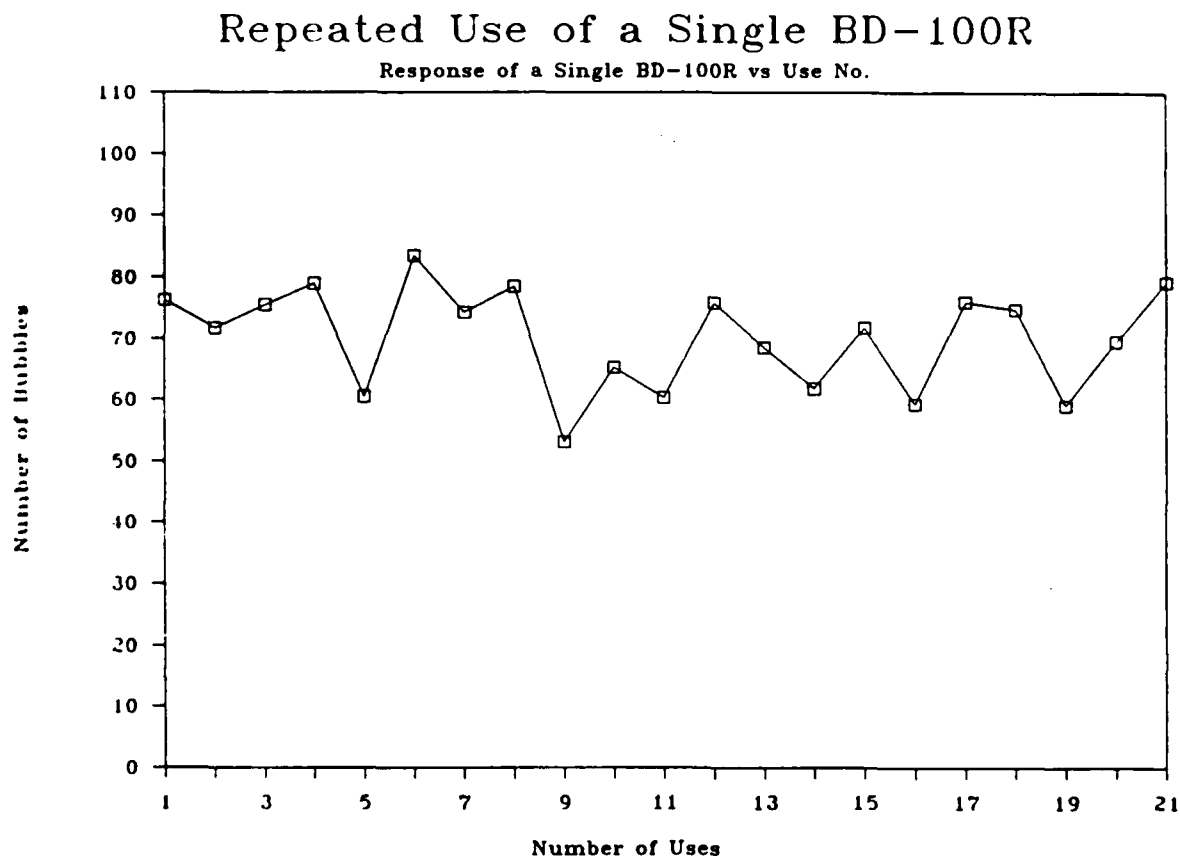


Figure 5.7 - Response of a single BD-100R for 21 uses.

All neutron induced reactions are statistical in nature because of the random manner in which nuclear events occur. Observations of nuclear events are known to fit a Poisson distribution. Therefore, the response of a radiation detection system should also fit a Poisson distribution. In order to determine if a series of measurements of the same field, made with the same detector fits a Poisson

distribution, the chi-square test can be performed on the data. The chi-square test indicates that the statistical distribution when making repeated readings of the bubble dosimeter should follow the relationship given by:

$$X^2 = \sum [(x_i - x_{av})/x_{av}] = nQ^2 \quad (5.1)$$

where:

$X^2$  = Chi-square parameter

$x_i$  = Number of bubbles in the  $i^{\text{th}}$  reading

$x_{av}$  = Mean number of bubbles observed over all  
readings

$n$  = Number of readings

$Q^2$  = Lexis divergence coefficient

The Lexis divergence coefficient in equation 5.1 is equal to unity for a Poisson distribution. For the 24 dosimeters studied in this part of the experiment, the divergence coefficient was determined as:

$$Q^2 = 0.98 \quad (5.2)$$

The result from equation 5.2 indicates that the bubble dosimeter roughly fits a Poisson distribution.

The mean responses of each group of six dosimeters, as shown in Figures 5.8 through 5.11, as expected show less percent variation from use to use than a single dosimeter. The error margins shown in the figures represent plus and minus one standard deviation within the group of six identically produced dosimeters. With the high passing rate

# Repeated Use of 6 BD-100R's (R/3.9)

43

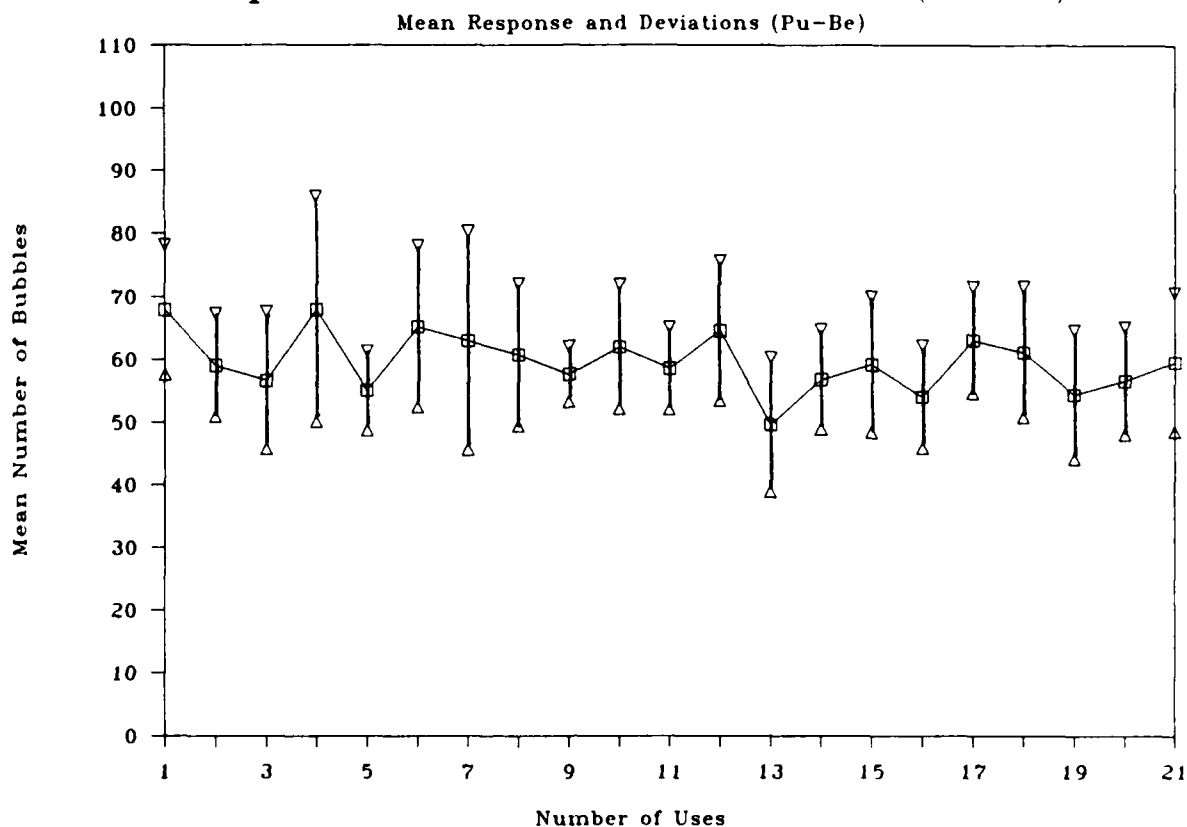


Figure 5.8 Repeated Use of 6 BD-100R's (Pu-Be) (R/3.9)

# Repeated Use of 6 BD-100R's (R/4.7)

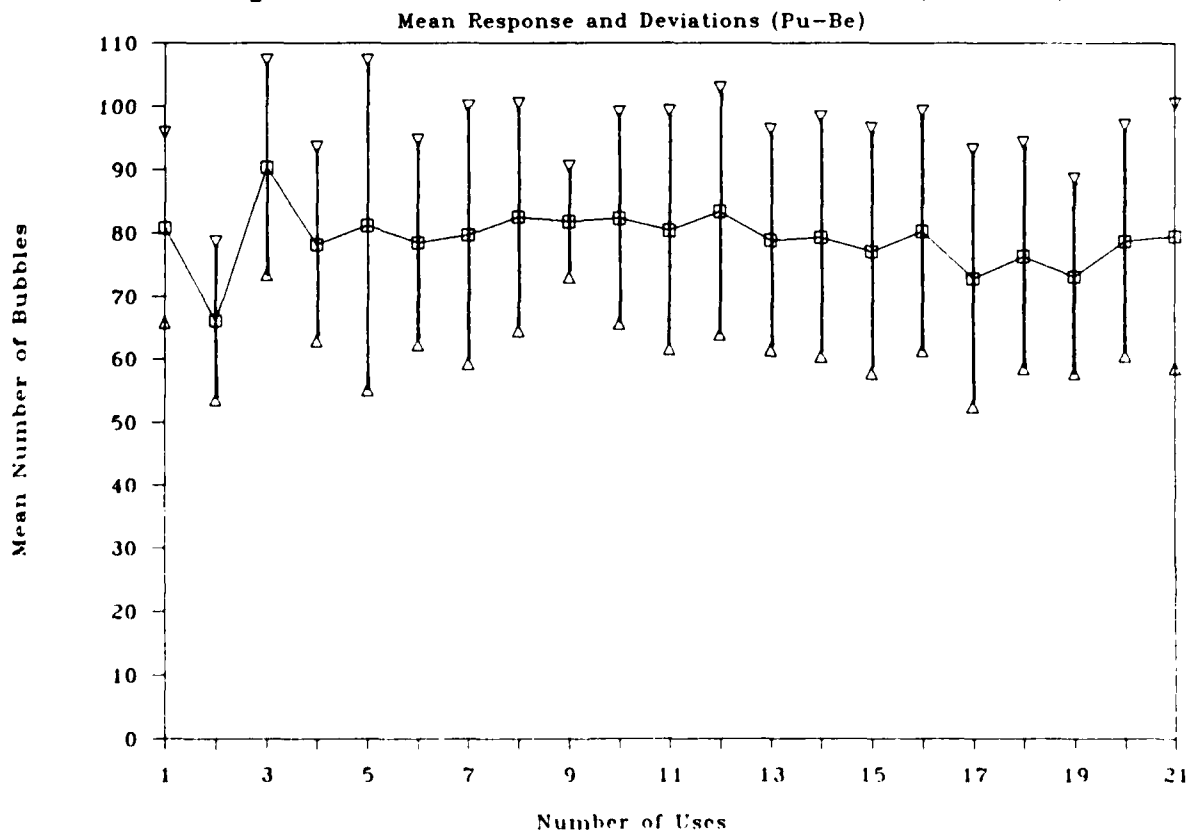


Figure 5.9 Repeated Use of 6 BD-100R's (Pu-Be) (R/4.7)

# Repeated Use of 6 BD-100R's (R/3.9)

44

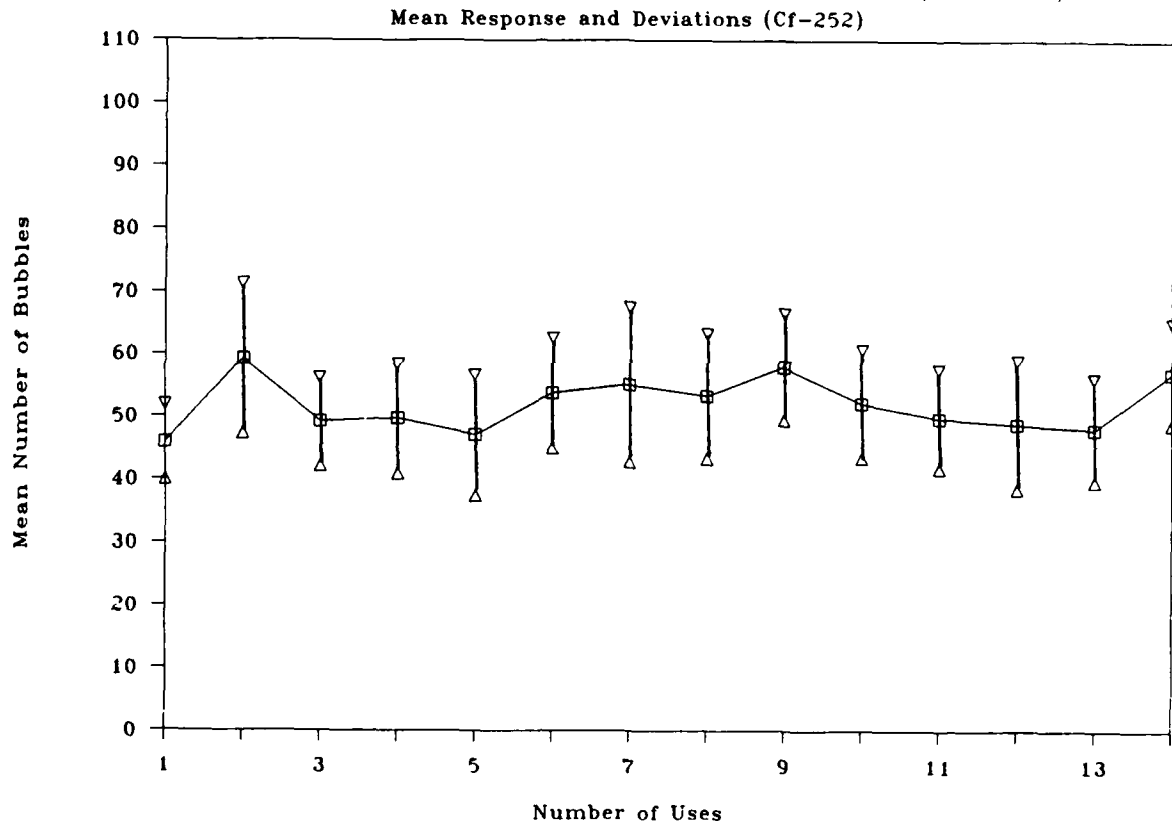


Figure 5.10 Repeated Use of 6 BD-100R's (Cf<sup>252</sup>) (R/3.9)

# Repeated Use of 6 BD-100R's (R/4.7)

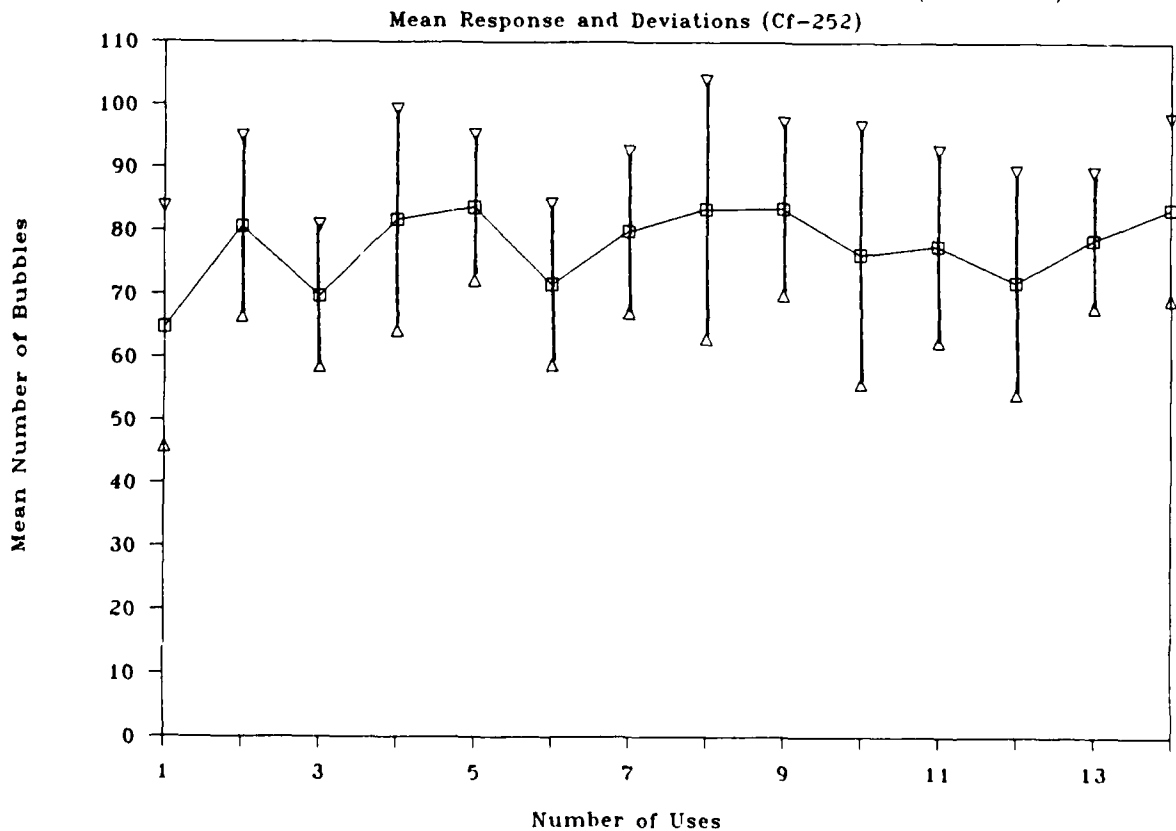


Figure 5.11 Repeated Use of 6 BD-100R's (Cf<sup>252</sup>) (R/4.7)



on the chi-square test, the large error margins can be attributed almost entirely to variations in the actual sensitivities of the individual detectors. This problem could be overcome by performing a calibration on each detector in order to determine its individual sensitivity, instead of using the manufacturer's listed value. This would yield a statistically well behaved detector with a verified sensitivity, independent of use number.

Although one set of dosimeters was run through 21 use cycles, that was not the end of the detector life. In fact there was no indication that the dosimeters were about to fail. This shows that from the re-use point of view, the BD-100R can be used as special purpose neutron dosimeter. Since many radiation workers are not exposed to large amounts of neutron radiation on a regular basis, a special neutron dosimeter could be used for high neutron exposure activities such as reactor fueling and nuclear weapons handling operations.

Since the bubble dosimeter is sensitive to temperature, it is important that the BD-100R be in thermal equilibrium with the environment before it is used to measure neutron dose. In order to prolong the shelf life of BD-100R's, they are stored in refrigerators, just above freezing. The thermal characteristics of the BD-100R, as it comes into equilibrium with its surroundings were therefore considered important. Several experiments were conducted to characterize the BD-

100R's transient thermal behavior.

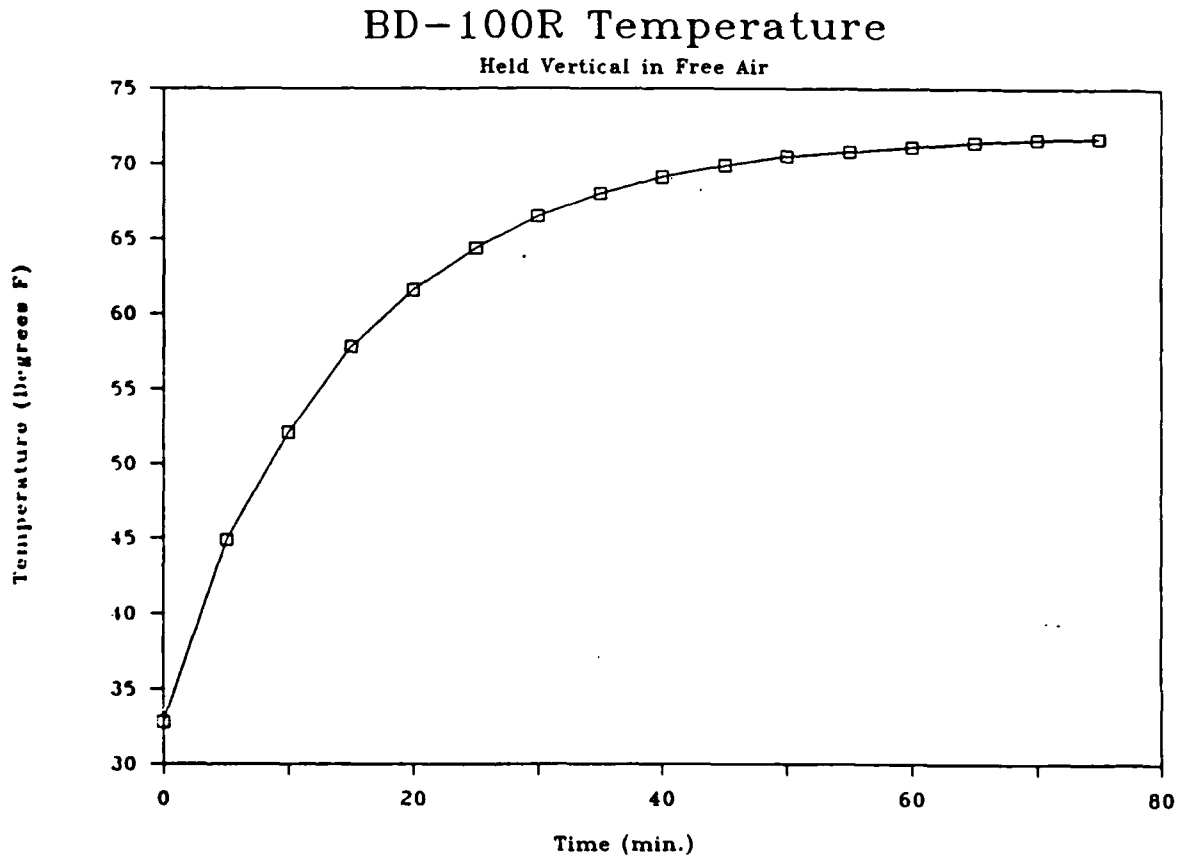


Figure 5.12 - Temperature response of the BD-100R as it warms to room temperature.

Figure 5.12 shows the temperature of a BD-100R over time as it is taken from cold storage up to room temperature under realistic conditions. A relationship was developed for the temperature (T) of the BD-100R on this curve, and is given by the equation:

$$(T_{\infty} - T)/(T_{\infty} - T_0) = e^{-0.064t} \quad (5.3)$$

where:

$T_{\infty}$  = Ambient air temperature, Fahrenheit or Rankine

$T_0$  = Cold storage temperature, Fahrenheit or Rankine

$t$  = Time (minutes)

Operationally, the most important implication of this characteristic of the BD-100R is the fact that the user has to wait almost an hour before full sensitivity is obtained.

## 6.0 BUBBLE SPECTROMETER PERFORMANCE

Spectrometers collect and unfold large amounts of neutron data by long and involved calculations, finally arriving at the energy dependent spectrum. Health physicists have been interested in the information these systems can provide because it would allow them to apply effective correction factors to existing dosimetry systems. One of the problems is that current spectroscopy systems, such as the NE-213, require extensive supporting electronics for data collection and processing. As a result, it has been difficult to obtain neutron spectral data outside of the laboratory.

The effective development of a portable neutron spectrometer based upon multiple threshold dosimeters would be an improvement in the field of neutron spectroscopy. A large portion of the U.S. Navy's research work in bubble dosimetry is presently attempting to determine the feasibility of the bubble spectrometer.

Work done at Chalk River during the last few years has produced the Bubble Detector Spectrometer (BDS), which uses six detectors with different liquids in order to achieve different energy response. The degree of superheat in a detector determines the minimum energy, or threshold, below which a detector will not respond. The thresholds for the six groups are 10 keV, 100 keV, 600 keV, 1500 keV, 2500 keV,

and 10000 keV. The individual detectors are correspondingly named BDS-10, BDS-100, etc. The original intention of those who did the developmental work on the BDS was to produce one of the detectors with a threshold in the 500 keV range. Problems in the fabrication of this detector led to its abandonment in favor of a detector with a lower threshold. The lower threshold detector was compensated with a Freon-114 overlay which yielded a detector with a threshold of 600 keV. All of the other detectors are used with no overlay, but a small amount of Freon-114 must be added to the BDS-600 each time it is used.

The procedure for unfolding the data collected with the BDS is a spectral stripping technique which is explained in detail in Appendix A. Each of the individual detectors has a listed sensitivity, and for each detector type there are cross-sections listed which show the relative response of the detector within each energy group. As the first phase of this analysis of the BDS system, a computer program was written to unfold BDS data using the listed sensitivities and cross-sections. Then the spectra that the BDS would be exposed to were determined. The neutron spectra for  $\text{Cf}^{252}$  and Pu-Be are well known, but due to neutron scattering effects, the spectrum from the 14 MeV neutron generator had to be calculated.

A very powerful analytical tool was employed for the calculation of the neutron spectrum at the location of the

irradiations. The Monte Carlo Neutron and Photon Transport Code System (MCNP), developed by Los Alamos National Laboratory, has the capability to predict the neutron spectrum at a given point.<sup>25</sup> The code simulates neutron interactions in the specifically defined materials and geometry of the environment surrounding both the neutron source and detector location. MCNP was obtained from the Radiation Shielding Information Center and installed on the U.S. Naval Academy's Gould computer system. A Monte Carlo Neutron-Photon (MCNP) problem was set up describing the 14 MeV neutron source, specifying the environmental geometry and materials. MCNP was then used to solve for the energy dependent spectrum. This solution is shown in Figure 6.1. The MCNP problem setup and procedures are given in Appendix B. The 14 MeV neutron spectrum was also unfolded using the NE-213 neutron spectrometer. This spectrum is shown in Figure 6.2.

The BDS was exposed to neutrons from  $\text{Cf}^{252}$ , Pu-Be, and the 14 MeV neutron generator. The irradiations were constrained by the BDS-10's response. Since, in theory, the BDS-10 should respond to all neutrons above 10 keV, it should give the largest reading of any of the detectors, when exposed to virtually any field. That fact, combined with the fact that the BDS-10 had the greatest listed sensitivity, about eight bubbles per millirem on average, meant that it should form considerably more bubbles than any of the other detectors. This was an important consideration because the irradiations

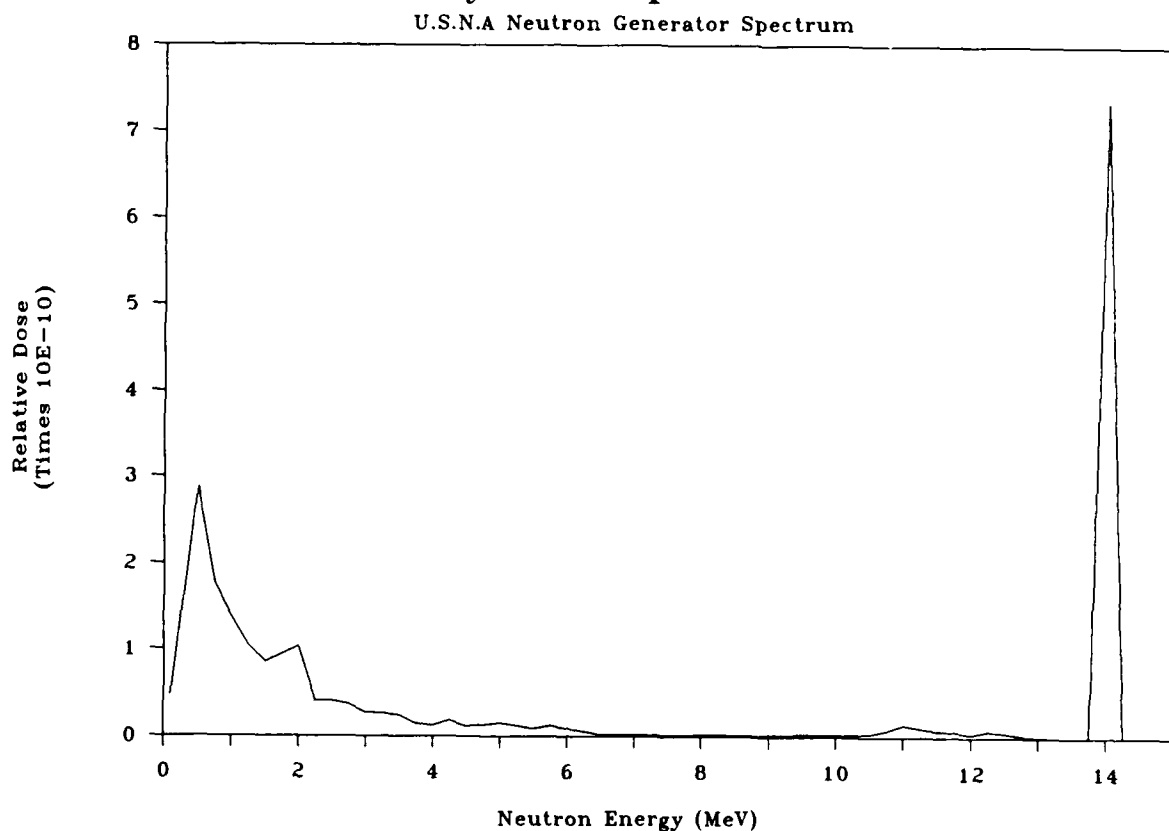


Figure 6.1 14 MeV Neutron Dose Spectrum

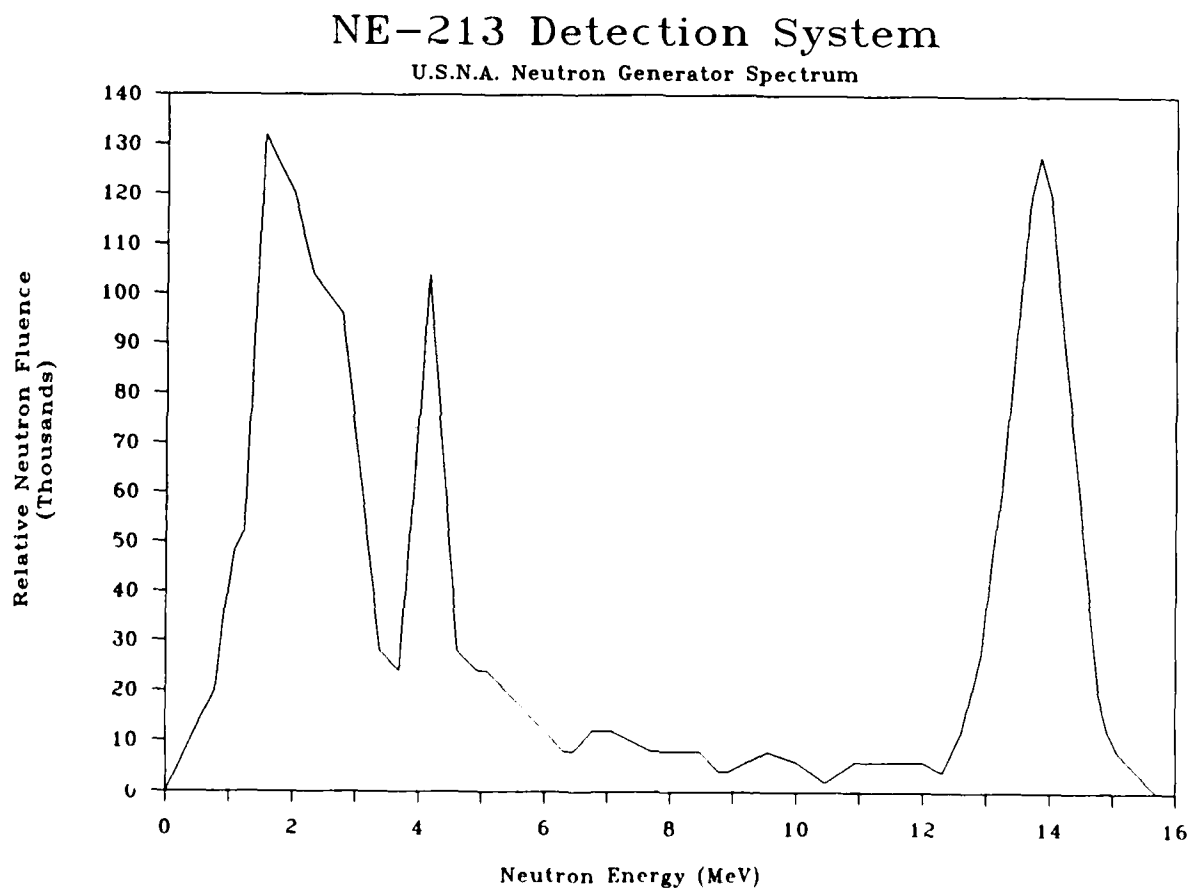


Figure 6.2 14 MeV Neutron Fluence Spectrum

had to be carefully timed to get statistically meaningful information from the other detectors and not cause a BDS-10 to form so many bubbles that it could not be read.

In every irradiation the BDS-10 responded lower than the theoretically calculated dose. The bubbles appeared large and were widely spaced. This could possibly be a quality control problem resulting from the detector liquid not being fully dispersed throughout the detector at the time of polymerization. Since  $\text{Cf}^{252}$  and Pu-Be do not produce many neutrons above 10 MeV, the BDS-10,000's generally did not respond significantly to those sources.

### Cf-252 Neutron Spectrum Measured by BDS

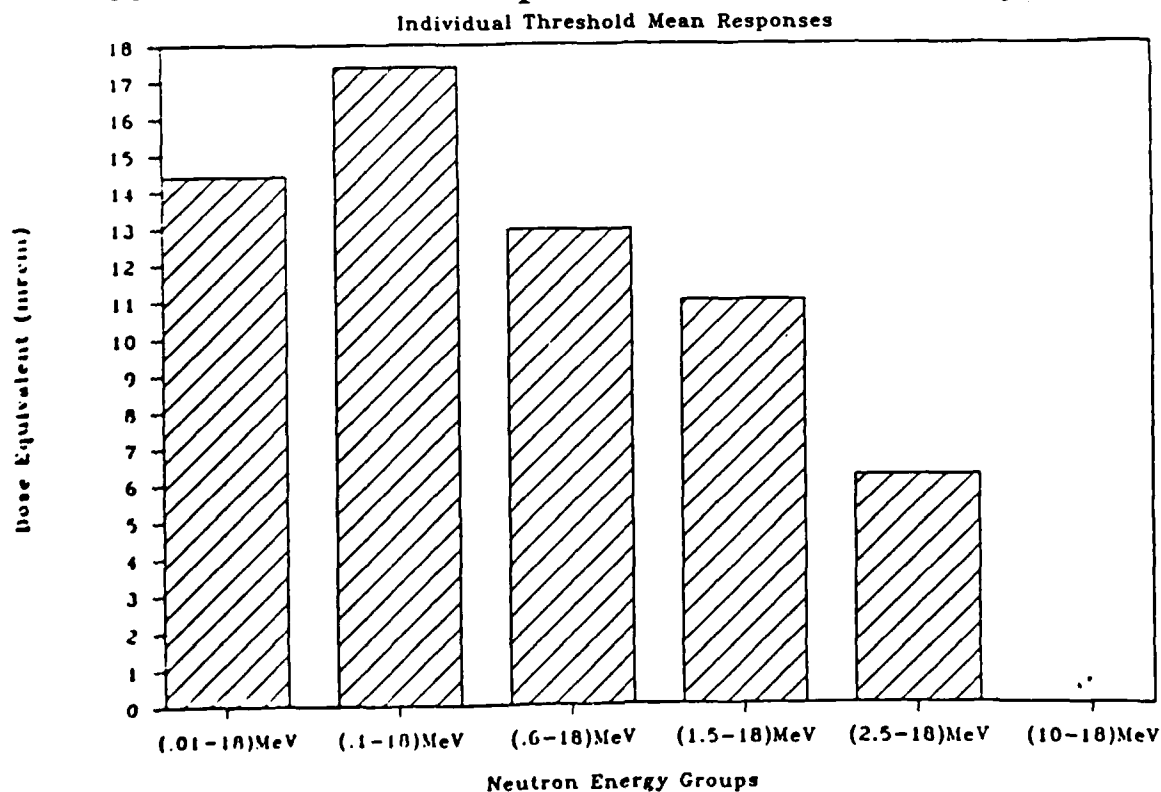


Figure 6.3 - Measured neutron doses for  $\text{Cf}^{252}$ .



For the 14 MeV neutrons, however, the BDS-10,000's responded considerably higher than the calculated dose at that energy.

Figure 6.3 shows dose as measured by the detectors in each of the six energy groups for  $\text{Cf}^{252}$ . It is clear that the reading in each higher energy group should be lower than the previous one, but this often was not the case. It was found that the BDS measures the  $\text{Cf}^{252}$  dose spectrum relatively well. Figure 6.4 shows the known unfolded fission spectrum of  $\text{Cf}^{252}$ .

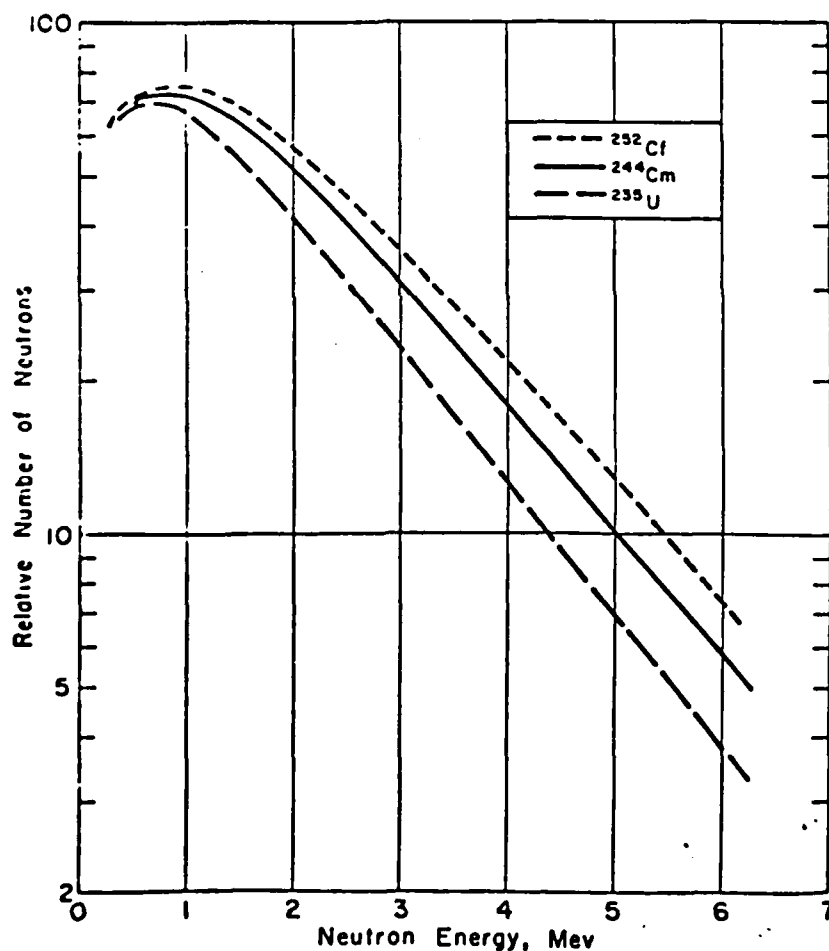


Figure 6.4 - Known  $\text{Cf}^{252}$  spectrum

When quality factors are applied and the dose is divided up into the six energy groups, the expected response of each detector can be calculated. This was done for the  $\text{Cf}^{252}$  and is shown in Figure 6.5. The theoretical calculated doses shown in Figure 6.5 are for the same energy groups as those measured with the BDS, shown in Figure 6.3.

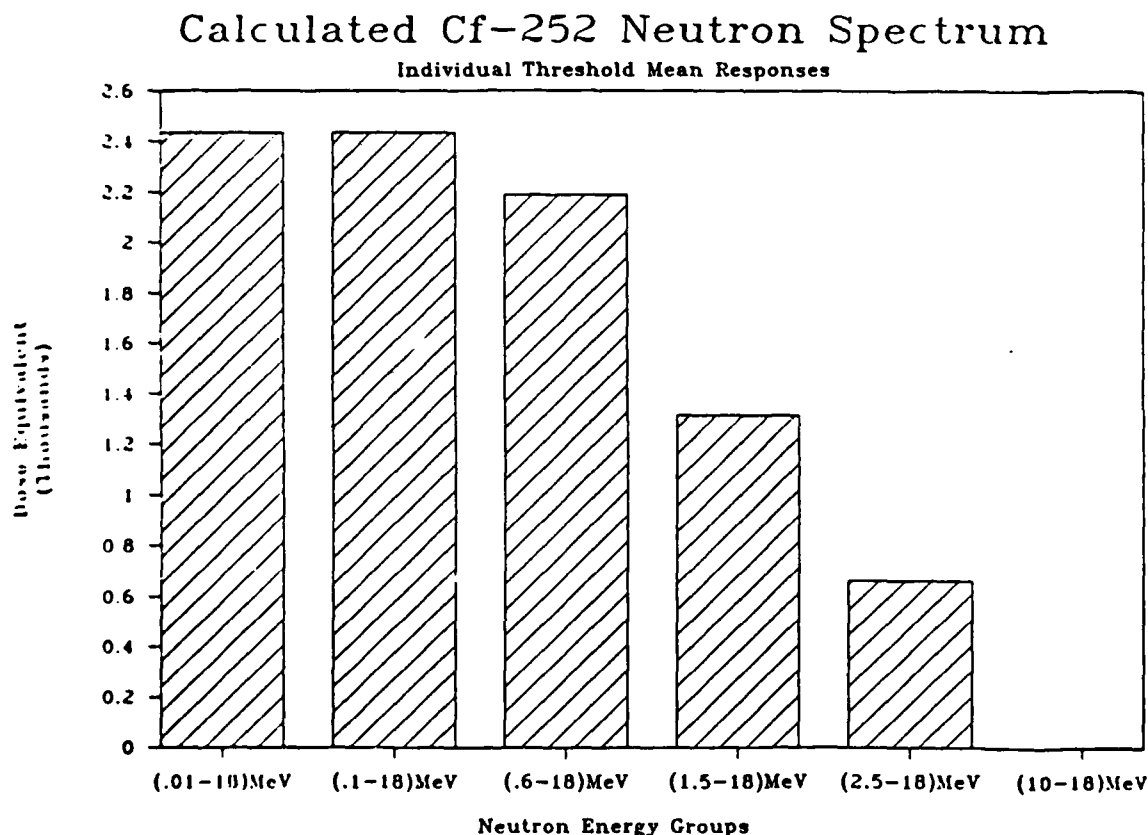


Figure 6.5 - Theoretical neutron doses for  $\text{Cf}^{252}$ .

Figure 6.5 shows the expected response of each of the six detectors, which agrees well with the measured response shown in figure 6.3. The  $\text{Cf}^{252}$  spectrum unfolded from the experimental data, as shown in Figure 6.6, shows a relative energy minimum in the 0.6 to 1.5 MeV range. This does not

correspond exactly with the fact that the  $\text{Cf}^{252}$  neutron peak energy is about 1 MeV. The large negative fluence recorded in the .01 to .1 MeV range appeared because of the impossible reading in the BDS-10, which carries through the unfolding

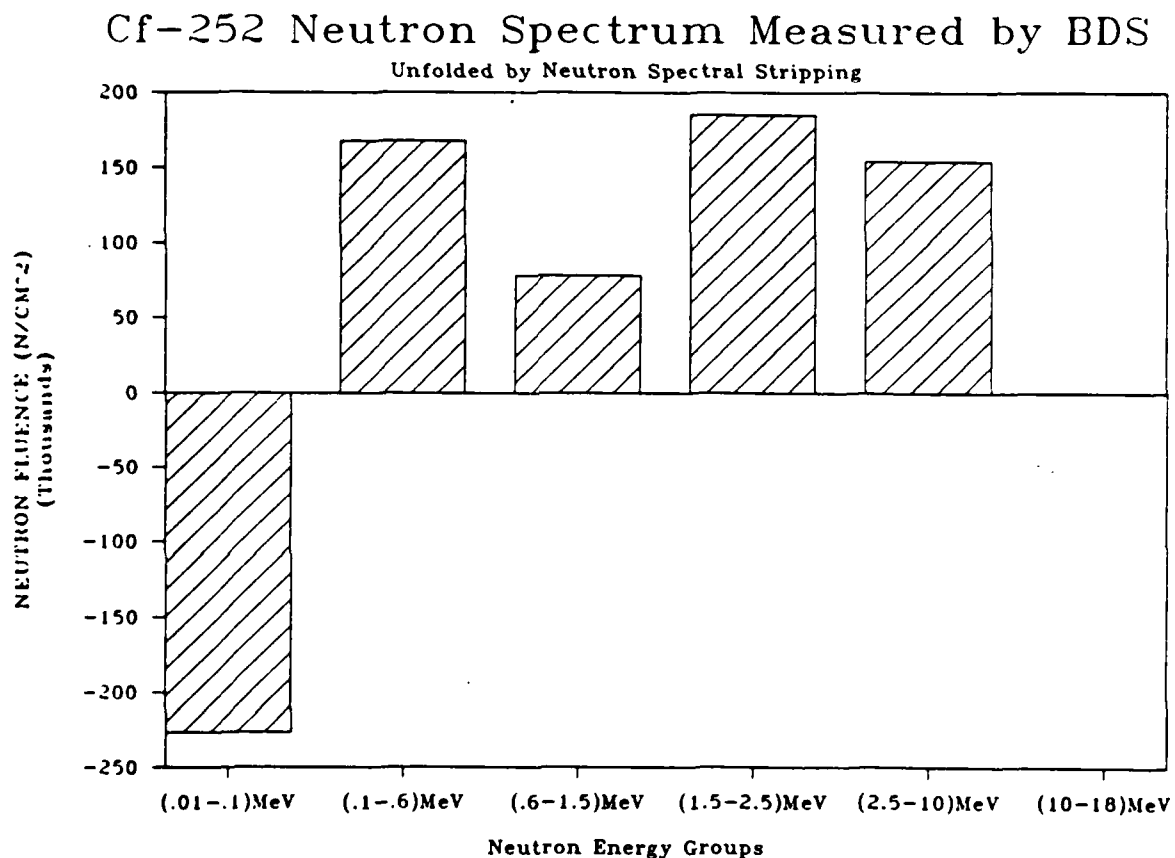


Figure 6.6 - Unfolded neutron spectrum for  $\text{Cf}^{252}$ .

procedure.

The BDS performance degraded as the energy of the neutron source increased. Because most of the neutron dose from Pu-Be falls between 2 and 4 MeV, BDS measurements of a Pu-Be source should be expected to show roughly equivalent readings in the first four energy groups. Figure 6.7 shows that two of the first four detectors responded with almost the same dose,

## Pu-Be Neutron Spectrum Measured by BDS

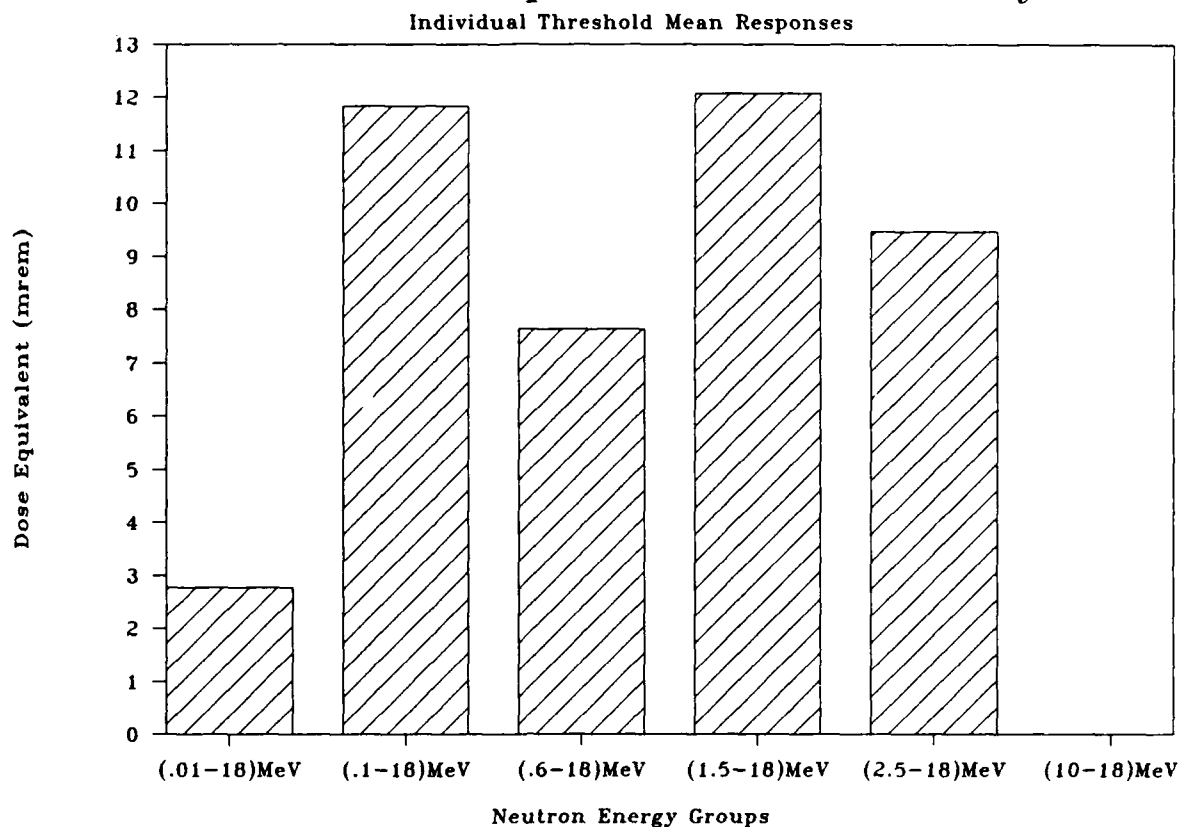


Figure 6.7 Measured Neutron Doses for Pu-Be

## 14 MeV Neutron Spectrum Measured by BDS

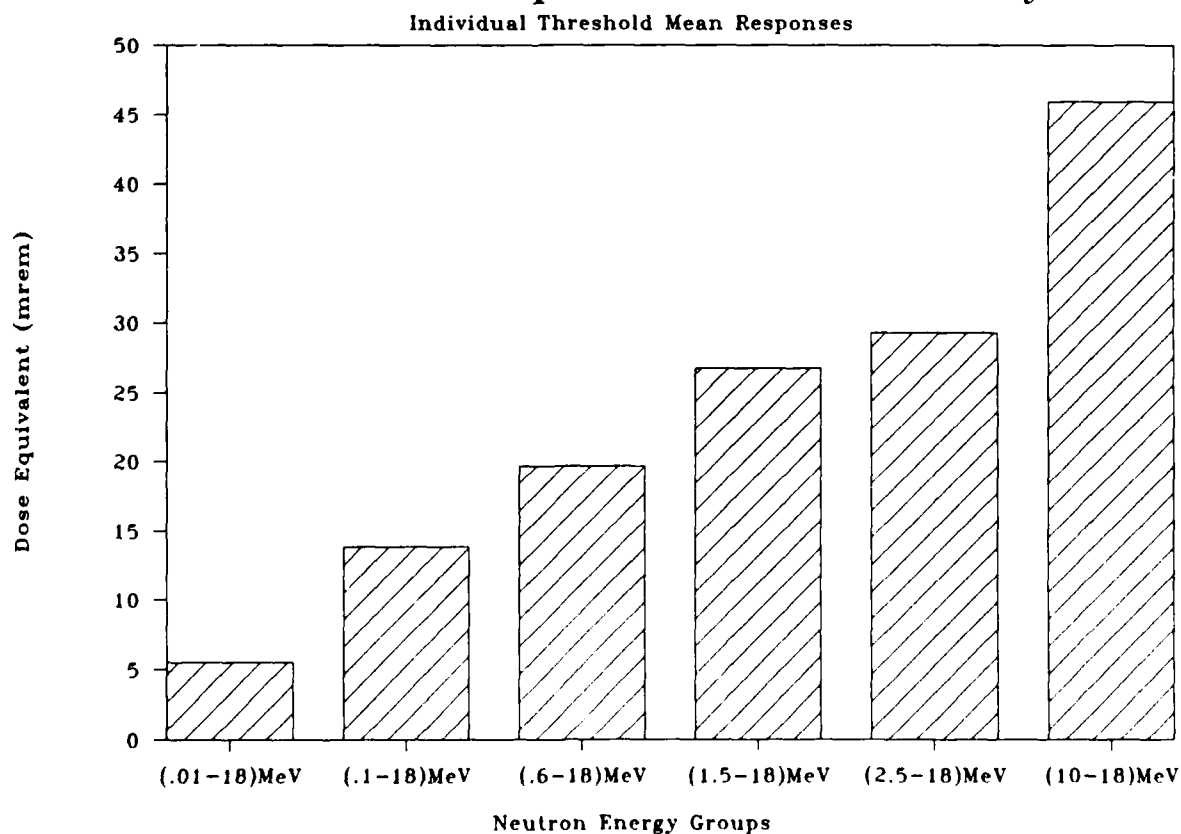


Figure 6.8 Measured Neutron Doses for 14 MeV

but the system showed an under-response in the first and third energy groups. Continuing this trend, the BDS shows a more severe under-response in the first five energy groups when exposed to neutrons from the 14 MeV neutron generator, as shown in Figure 6.8. The highest threshold detector was also found to over-respond to the high energy neutrons approximately by a factor of two.

The number of impossible readings obtained from the Pu-Be and 14 MeV irradiations account for the large errors and negative fluences encountered in the unfolded spectra shown in Figures 6.9 and 6.10. The spectral stripping technique for neutron spectrum unfolding is also responsible for part of the error. These figures are representative of over a total of 20 BDS irradiations, none of which yielded accurate spectral data.

Each of the spectrometer sets was re-used several times with no significant sensitivity changes observed. Four of the twelve BDS-600 detectors did not survive. After a few use cycles, BDS-600's began to eject the detector material from the tube when opened after reading and prior to pressurization. This was probably caused by some of the Freon-114 overlay getting trapped under the detector material and building up pressure when the detector was opened. Another problem that persisted throughout the evaluation of the spectrometer was the fact that many detectors were cloudy. The BDS-10,000's had the lowest detector clarity, which

## Pu-Be Neutron Spectrum Measured by BDS

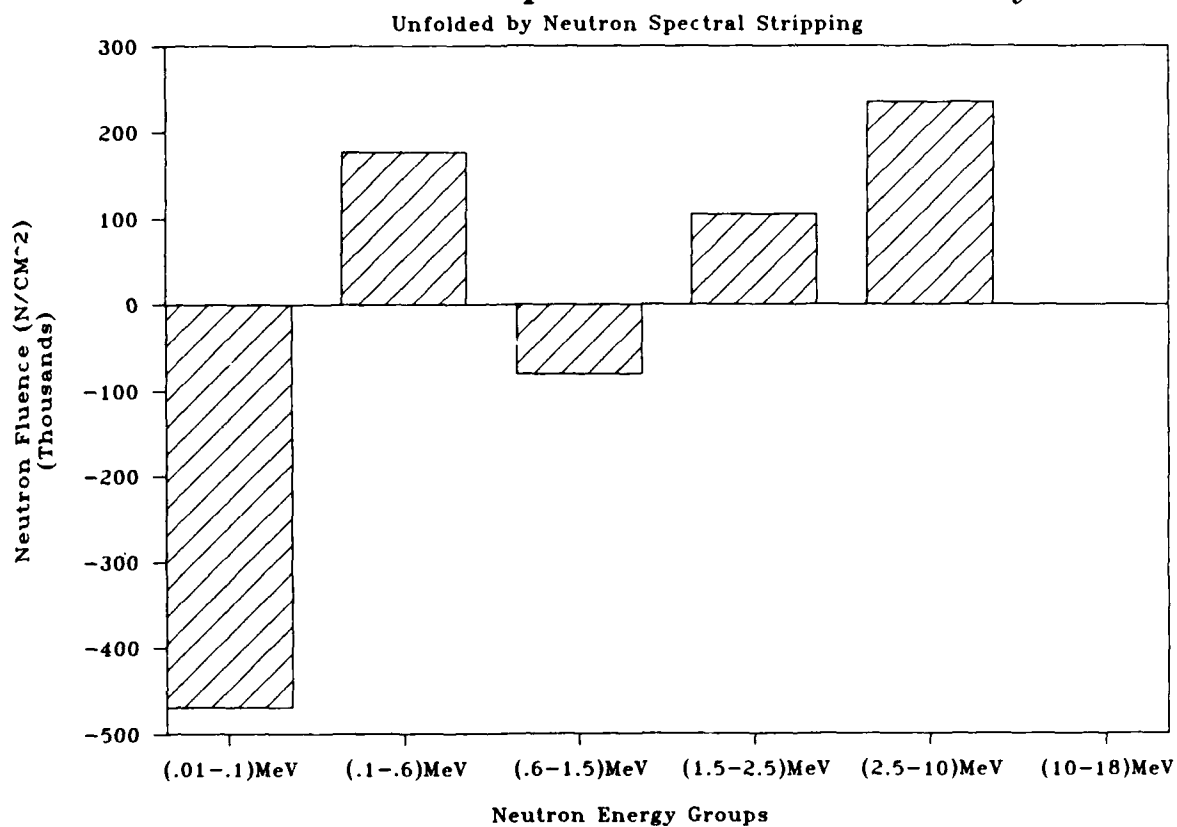


Figure 6.9 Unfolded Neutron Spectrum for Pu-Be

## 14 MeV Neutron Spectrum Measured by BDS

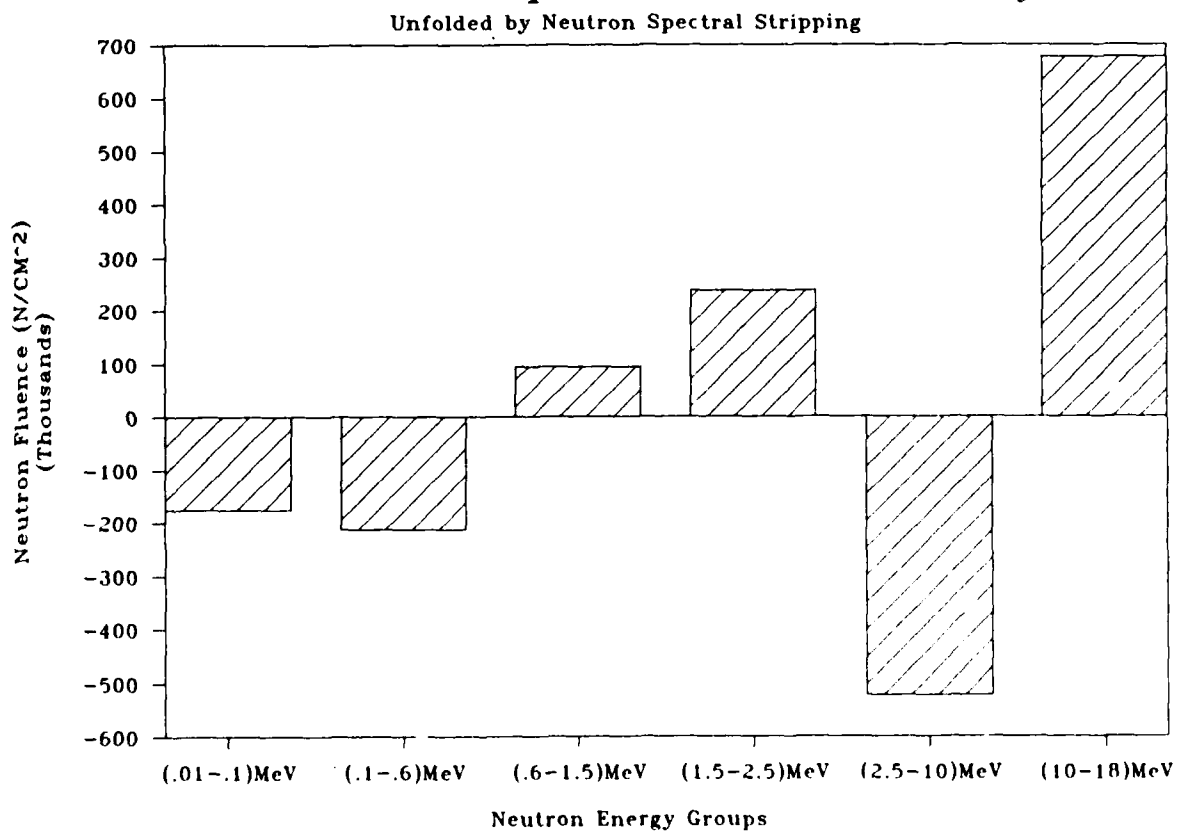


Figure 6.10 Unfolded Neutron Spectrum for 14 MeV

worsened as they were reused. Eventually, after eight uses over a period of two weeks, the detectors could not be read. The detectors finally failed completely after about two weeks because the detector material began leaking out of the tubes. Over time, the material gradually expanded, eventually to the point that the tubes could not be resealed. When the spectrometer sets were evaluated they were between five and seven months old. It is possible that the poor results were obtained because the sets were simply past their effective shelf-life.

## 7.0 DETECTOR COMPARISONS

Concurrent with the BD-100R or BDS-100 irradiations, other conventionally accepted means of neutron detection were performed side by side with the bubble dosimeters. The objective was to quantify the response of the bubble dosimeter, relative to standard detection systems, in varying neutron fields. For the  $\text{Cf}^{252}$  and Pu-Be the theoretical dose was also calculated. This was done by determining the current activity of the source, applying an average quality factor based upon that source's known neutron spectrum, and then multiplying by the spatial attenuation factor ( $1/4\pi r^2$ ). Because of the proximity of the sources and detectors, most of the neutron flux was believed to be uncollided, therefore neutron scattering effects were neglected.

The detection systems used were the neutron rem-meter (A/N-PDR-70), the TLD, the TEPC, CR-39 foils, and the NE-213. All of these systems measure dose equivalent except for the NE-213 which integrates the absorbed dose. In order to convert the absorbed dose as measured by the NE-213 to dose equivalent, an average quality factor was applied. The neutron spectra for  $\text{Cf}^{252}$  and Pu-Be were known, and to account for room scattering, the neutron spectrum from the 14 MeV



neutron generator had to be determined analytically, using the MCNP computer code. For  $\text{Cf}^{252}$  and Pu-Be, the ICRP quality factors were applied to the known spectra to obtain an average quality factor for the source. For the neutron generator, the fraction of the total dose at each energy, as determined using the MCNP spectral solution, was multiplied by the neutron quality factor at that energy. These products were summed to obtain the average neutron quality factor across the entire spectrum for the neutron generator field.

The TLD's and the CR-39 foils used in these experiments were read by the U.S. Naval Medical Command's Naval Dosimetry Center and the Nevada Test Site, respectively. Both the TLD and the CR-39 require a spectrum correction factor to compensate for their non-linear response. In the case of the TLD, the default correction factor of 10 was applied. This factor is used for unknown spectra and theoretically yields the most conservative estimation of dose. The CR-39 foils are calibrated against a Pu-Be source, so the correction for the Pu-Be spectrum is unity. For the 14 MeV spectrum, the Nevada Test Site uses a correction factor of 2.38.<sup>26</sup>

Table 7.1 shows a comparison of the various detection system responses relative to the BD-100R for irradiations done with the 14 MeV neutron generator. The relative response is the ratio of the comparison detector response to the bubble dosimeter response.

**TABLE 7.1 - RELATIVE RESPONSES TO 14 MeV NEUTRON GENERATOR**

<u>DOSIMETER</u>	<u>RELATIVE RESPONSE</u>
A/N-PDR-70	1.01
TLD	1.75
TEPC	1.48
CR-39	0.97
NE-213	1.36

As shown in Table 7.1, the bubble dosimeter was found to have a response equivalent to that of the A/N-PDR-70 and the CR-39. The A/N-PDR-70 and CR-39 under-respond to high energy neutrons by about a factor of 2.5. Since the bubble dosimeters had an equivalent response, they may also be under-responding in this region. The bubble dosimeters were found to under-respond relative to the TLD, TEPC, and NE-213.

Results of irradiations with Pu-Be are shown in Table 7.2.

**TABLE 7.2 - RELATIVE RESPONSES TO Pu-Be NEUTRONS**

<u>DOSIMETER</u>	<u>RELATIVE RESPONSE</u>
A/N-PDR-70	1.34
TLD	0.30
TEPC	0.93
CR-39	1.24
NE-213	2.07
THEORETICAL	1.16

As shown in Table 7.2, the bubble dosimeter tended to respond lower than the A/N-PDR-70, CR-39, NE-213, and the theoretically expected dose. In this energy range, the bubble dosimeter responded in the same manner as the TEPC. In these exposures, the doses received by the TLD's were close to the device's lower limit of detection, possibly resulting in the

TLD under-response. A limited amount of data was obtained with the NE-213 for the Pu-Be source. This results in a lower level of certainty for the NE-213 data in Table 7.2.

**TABLE 7.3 - RELATIVE RESPONSES TO  $\text{Cf}^{252}$  NEUTRONS**

<u>DOSIMETER</u>	<u>RELATIVE RESPONSE</u>
A/N-PDR-70	1.46
TLD	0.19
TEPC	0.95
THEORETICAL	1.07

Table 7.3 shows that in this lower energy range, the bubble dosimeter response is consistent with that of the TEPC and the theoretical dose. The bubble dosimeter under-responded slightly with respect to the A/N-PDR-70. The largest difference was found with the TLD, however, again the total doses ranges between only 18 and 50 mrem.

## 8.0 CONCLUSIONS AND RECOMMENDATIONS

The automatic optical reading system made the rapid counting of large numbers of dosimeters possible. The effective upper limit, in terms of the number of bubbles readable with the system, was found to be about 110, which extends the dynamic range by about a factor of two over manual reading. The most accurate results were obtained from the average of four counts at different angles with a computer enhancement of 95 to 100. The biggest problem in the optical counting of a bubble dosimeter is the fact that bubbles tend to obscure other bubbles at high bubble concentrations. If the size of the individual bubbles were reduced, the number of bubbles that could be effectively counted could be increased. Another option would be to change the shape of the detector itself. If a wider and thinner shaped tube were employed, the two dimensional projection used in the counting routine would be a closer approximation of the real image. Other counting systems, such as that currently under development at Chalk River, have the potential to substantially extend the dynamic range of the bubble dosimeter.

The number of bubbles formed in a BD-100R was found to increase over the first fifteen hours after irradiation.

Since over a third of the final reading appears at the time of irradiation, the bubble dosimeter could serve as an adequate indication of the presence of high levels of neutron radiation.

During 21 uses of a single BD-100R, no changes in sensitivity were observed. At the 21st use cycle, the BD-100R was still performing well and there is no reason to believe that it was near the end of its useful life. This confirms the usefulness of the BD-100R as a special purpose dosimeter for use during periods of expected high neutron exposure. The individual sensitivities of the BD-100R's show substantial variation, and appear to require calibration prior to use. The BD-100R responded statistically as expected.

The Bubble Detector Spectrometer shows a good deal of promise if the problems with the individual detector sensitivities can be overcome. Good results were obtained for irradiations with  $\text{Cf}^{252}$ , but irradiations with Pu-Be and 14 MeV neutrons yielded poor results. To obtain a better idea of the response characteristics of the individual detectors they should probably be irradiated with a series of well calibrated monoenergetic neutron beams from an accelerator.

Comparisons of the BD-100R with several other detection systems show that it behaves well over a wide range of neutron energies and that its readings are fairly consistent with currently accepted systems.

#### ACKNOWLEDGEMENTS

The Naval Medical Command Research and Development Center provided the financial support for this project. I would like to take this opportunity to thank LCDR H.F. Kershner for his direction and leadership. From the Naval Surface Warfare Center, White Oak, Dr. Gordon Reil provided technical assistance and valuable discussions. Dr. Bob Schwartz and Dr. Charlie Eisenhauer, from the National Institute of Standards and Technology, provided hardware assistance and insight on MCNP operation. CDR Bob Devine and LCDR Paul Blake, from the Dosimetry Center, provided assistance with TLD's, and Joe Wells, from the Nevada Test Site, helped with the CR-39 readings. Here at the Naval Academy, Jim Harle, from computer services, made MCNP run smoothly. Marie Harper, from Nimitz Library, managed to obtain every reference requested, even the most obscure. Last, and certainly not least, I would like to thank Mike Gibbons for his unending help in the nucleonics laboratory with all aspects of the research.

## REFERENCES

1. "Protection against Ionizing Radiation from External Sources," International Commission on Radiological Protection, Report 21. 1977.
2. L. Tomasino, "Recent Trends in Radioprotection Dosimetry: Promising Solutions for Personal Neutron Dosimetry," Nuclear Instruments and Methods in Physics Research. A255, pp. 293-297. 1987.
3. S.C. Roy, R.E. Apfel, Y.C. Lo, "Superheated Drop Detector: A Potential Tool in Neutron Research," Nuclear Instruments and Methods in Physics Research. A255 pp. 199-206. 1987
4. H. Ing, "Novel Inexpensive Neutron Detector (BD-100)," Technical Note, Chalk River Laboratory. 1987
5. R.V. Griffith, "Review of the State of the Art in Personnel Neutron Monitoring with Solid State Detectors," Proceedings of the Sixth Symposium on Neutron Dosimetry, Neuherberg, Germany. 1987
6. D.A. Glaser, "Some Effects of Ionizing Radiation on the Formation of Bubbles in Liquids," Physical Review. Vol. 87. No. 4. p. 665. 1952
7. M.G. Millet, "An Evaluation of the BD-100R Neutron Dosimeter," Master's Thesis, University of Maryland. 1988
8. M.G. Millet, F. Munno, D. Ebert, M.E. Nelson, "An Evaluation of the BD-100R Neutron Bubble Dosimeter's Sensitivity to Neutron and Gamma Sources in Mixed Fields," Proceedings of the 22nd Topical Meeting on Instrumentation. The Health Physics Society. pp. 222-230. 1988.
9. R.E. Apfel, S.C. Roy, Y.C. Lo, "Prediction of the Minimum Neutron Energy to Nucleate Vapor Bubbles in Superheated Liquids," Physical Review A. Vol. 31. No. 5. pp. 3194-3198. 1985.
10. F. Seitz, "On the Theory of the Bubble Chamber," The Physics of Fluids. 1. pp. 2-13. 1958.
11. H. Ing, H.C. Birnboim, "Bubble-Damage Polymer Detectors for Neutron Dosimetry," Proceedings of the Fifth Symposium on Neutron Dosimetry. Munich, Germany. pp. 883-894. 1984

12. H. Ing, K. Tremblay, "To Develop a Set of Variable Lower-Energy Threshold Neutron Detectors for Use as a Spectrometer," Canadian Department of Defense Report. February 29, 1988.
13. "Exposure Meters and Dosimeters - General Methods for Testing," ISO International Standard 4071. 1978.
14. H. Ing, "The Status of the Bubble Damage Polymer Detector," Nuclear Tracks. Vol. 12. pp. 49-54. 1986
15. N.E Ipe, D.D Busick, R.W. Pollock, "Factors Affecting the Response of the BD-100 and a Comparison to CR-39," Proceedings of the Sixth Symposium on Neutron Dosimetry. Neuherberg, Germany. 1987.
16. H. Ing, W.G. Cross, P.J. Bunge, "Spectrometers for Radiation Protection at Chalk River Nuclear Laboratories," Radiation Protection Dosimetry. Vol. 10. No. 1-4. pp. 137-145. 1985
17. C.A. Perks, R.T. Devine, K.G. Harrison, R.J. Goodenough, J.B. Hunt, T.L. Johnson, G.L. Reil, R.B. Schwartz, "Neutron Dosimetry Studies Using the New Chalk River Nuclear Laboratories Bubble-Damage Detector," Proceedings of the Sixth Symposium on Neutron Dosimetry. Neuherberg, Germany. 1987.
18. H.H. Rossi, W. Rosenweig, "A Device for the Measurement of Dose as a Function of Specific Ionization." Radiology, Vol. 64, 404, 1955.
19. R.J. Hilardes, "Development of a Tissue Equivalent Proportional Counter System for the Measurement of Neutron Dose," United States Naval Academy - Trident Scholar Report, No. 145. 1987.
20. R.T. Devine, M. Moscovitch, P.K. Blake, "The U.S. Naval Medical Command Thermoluminescent Dosimetry System," U.S. Government Report. 1989.
21. "Department of Energy Standard for the Performance Testing of Personnel Dosimetry Systems," DOE/EH-0027, U.S. Government Printing Office, December, 1986.
22. M.E. Nelson, D.A. Miller, P.F. Wiggins, G. Riel, T.D. Strickler, "Computer Graphics to Separate Neutron From Gamma-Ray Spectra, Applied to the Measurement of Neutron Attenuation Coefficients Using an NE-213 Scintillator," Nuclear Technology Vol. 71. pp. 512-519. Nov. 1985.
23. C. Fischahs, "Theory and Operation of the NE-213 Detector and ND9900 Analyzer," U.S. Naval Academy EN 495 Research Project Report, December, 1988.



24. R.D. Evans, The Atomic Nucleus, McGraw-Hill, New York, 1955.
25. "Monte Carlo Neutron and Photon Transport Code System," Version 3A. RSIC code package CCC-200. Los Alamos National Laboratory, Los Alamos, New Mexico.
26. Personal communication with J. Wells, Nevada Test Site, April, 1989.

## APPENDIX A

### THE SPECTRAL STRIPPING METHOD FOR BDS NEUTRON UNFOLDING

Many sophisticated methods exist for the unfolding of neutron data, in order to obtain the energy dependent neutron spectrum. Most of these methods require powerful computers to do the involved mathematical calculations. Spectral stripping is one of the most basic methods of spectral unfolding, but has some drawbacks. The primary advantage of the spectral stripping method is the fact that it is possible to do all of the calculations with a hand-held calculator, for a system with a small number of threshold measurements. This is an important feature for a portable spectroscopy system, because the user in the field or at sea would probably not have sophisticated computers available to run large unfolding codes. The most significant drawback of the spectral stripping method is the manner in which errors propagate through the calculations. As the calculations proceed, the errors from the higher energy groups accumulate in the lower energy groups, resulting in lower degrees of certainty. Figure 6.6 clearly illustrates this effect. If the spectral data are only intended to be used for purposes such as correcting neutron dose from other measurement systems, this

method may be useful.

For the BDS, since only six thresholds of detection are presently available, a six-group histogram is used to approximate the spectrum. The neutron fluence in each energy group is the final result of the unfolding procedure. Neutron fluence ( $N$ ) (neutrons/cm<sup>2</sup>) can be defined as:

$$N = \phi t \quad (A.1)$$

where:

$$\phi = \text{Neutron flux, (neutrons/cm}^2 \text{ sec)}$$

$$t = \text{Time, sec}$$

In each of the six energy regions, neutron fluence per unit energy is assumed constant. The fluence in each energy group can be found using the following procedure:

1. For each of the six thresholds, the average number of bubbles in all detectors which have the same threshold is determined ( $A_i$ ), where  $i = 1$  to 6, corresponding to the BDS-10 through BDS-10,000 respectively.

2. Normalize the responses  $A_i$ , to unit sensitivity by dividing by the detector's listed sensitivity:

$$R_i = A_i / \text{sensitivity} \quad (A.2)$$

This gives the dose recorded by each detector.

3. Calculate the fluence,  $(N_6)$ , in the sixth (highest) energy group, 10 to 18 MeV, from:

$$R_6 = \sigma_{66} \times N_6 \quad (\text{A.3})$$

where  $\sigma_{66}$  is the average response of the BDS-10,000 over the energy range 10 to 18 MeV. Values of  $\sigma_{ij}$  are given in table A.1 for the six energy groups.

4. Calculate the fluence in the fifth energy group, 2.5 to 10 MeV, from:

$$R_5 = (\sigma_{55} \times N_5) + (\sigma_{56} \times N_6) \quad (\text{A.4})$$

5. In the same manner, calculate the fluence in each of the four remaining energy groups.

TABLE A.1

BDS Average Cross-Sections ( $\sigma_{ij}$ ) Over Six Energy Groups

Group	1	2	3	4	5	6
Energy (Mev) (.01-.1) (.1-.6) (.6-1.5) (1.5-2.5) (2.5-10) (10-18)						
Detector:						
BDS-10	2.30e-5	4.27e-5	3.72e-5	3.10e-5	2.47e-5	3.04e-5
BDS-10	-	2.49e-5	3.23e-5	3.50e-5	2.73e-5	3.25e-5
BDS-600	-	-	2.54e-5	3.95e-5	2.37e-5	2.99e-5
BDS-1500	-	-	-	2.65e-5	3.97e-5	6.08e-5
BDS-2500	-	-	-	-	4.04e-5	7.44e-5
BDS-10000	-	-	-	-	-	6.78e-5

## APPENDIX B

### Monte Carlo Neutron and Photon Transport Code System

MCNP is a general Monte Carlo code for neutron and photon transport. MCNP simulates particle transport in a geometric configuration of materials. The materials are grouped into cells which are bounded by first degree surfaces (i.e. planes) and second degree surfaces (i.e. spheres, parabolas, etc.). The nature and position of the radiation source, the materials, the surface equations, and the cells must all be specifically defined by the user. Through a complex and semi-random process, MCNP determines the path of each particle from its birth in the radiation source until it is absorbed, escapes the defined geometry, or is killed by some other user defined criteria. From this type of analysis, the code is capable of estimating the entire energy dependent spectrum at any point within the geometry.

MCNP, developed by Los Alamos National Laboratory, Los Alamos, New Mexico, is available through the Radiation Shielding Information Center, Oak Ridge, Tennessee. Version 3A is operational on the U.S. Naval Academy's Gould computer system, along with extensive material cross-section data.

The problems recently run at the U.S. Naval Academy dealt primarily with the determination of the neutron spectrum in the nucleonics laboratory irradiation room, at a point 150 cm.

from the neutron generator. In order to run an MCNP problem, the user creates an input file which is read by the code. In the first section of the input, the cells are defined, using the surfaces defined in the second section of the input. For the problems run in the recent studies, the surfaces of all of the walls were approximated by planes. Items such as small metal tables, power supplies, and electronic equipment in the irradiation room were neglected. It is important that there be no discontinuities in the cell definition because that will cause the code to lose track of too many particles.

The third section of the input is used for source definition, material definition, and other user defined options. The source was defined as a monoenergetic 14 MeV neutron source. The materials were defined from Los Alamos data on concrete, which was used in the construction of the walls, floor, and ceiling of the irradiation room. The air was approximated as a void because of the low probability of neutron interaction. One of the options defined was the detector type and location. A point detector, at the location where the bubble dosimeters were always situated, was chosen. The detector is also defined by the energy ranges, or bins, which it measures. These were chosen to give good coverage of the ranges important to dosimetry. The number of particles run through the geometry and tallied before the program stops can also be defined. It is important that the number of particles run is large enough for the figure of merit to

stabilize.

The neutron cross-sections are stored in libraries which the code accesses. The libraries used in these studies were ENDF/B-III, ENDF/B-IV, and LLL-Howerton.